Addis Ababa University

Addis Ababa Institute of Technology

School of Mechanical and Industrial Engineering

Identification of the Best Material Combination Between Wheel and Rail of Railway Vehicle with Minimum Wear Rate

A Thesis Submitted to the School of Mechanical and Industrial

Engineering in Partial Fulfillment of the Requirements for the Degree

Of Masters of Science in Mechanical Engineering

By: Natnael Tesfamichael

Advisor: Ato Habtamu Tekubet

March 2015

ACKNOWLEDGEMENT

First, I would like to thank God for his endless love and support. Next, I would like to express my deepest gratitude for my adviser, Ato Habtamu Tekubet for his interest in this thesis subject, for his helpful comments and suggestions and without whose advises, encouragement and patience, this work would not have been possible. The suggestions, tips and advises given by my friend Fisha Mengesteab were immensely helpful in modeling the railway vehicle. I would like to express my sincere thanks to Prof.S.H. Luo for his humble approach, he also guides me on the result analysis of the SIMPACK vehicle model.

Finally, I want to thank my family and friends for their support and encouragement.

Thank you all!

ABSTRACT

Wear is a natural phenomenon that exists when two bodies, which are in contact, perform a relative motion; this is also true for the wheel and rail of a railway vehicle. This wear is mainly dependent on the type of material they are made of. There is a tolerable level of wear that is safe to the railway operation. Once this critical wear level is reached, it is mandatory to re-profile the wheel, grind the rail. However, after some time it will be worn out to the level it can no more be used and the whole system must be replaced with a new one. This indicates that there is a need to focus on the wear properties of wheel and rail materials in order to secure a safe and sustainable railway operation.

This research tries to set new combinations (pairs) of wheel and rail materials, simulate them for wear performance using a multi body simulation software (SIMPACK). An important criteria for the comparison is the hardness and strength of the wheel/rail materials. Then compare the wear rate of the different combination and identify for the best material combination with the minimum wear rate. Based on the simulation it is found that a softer wheel material rolling on a relatively harder rail material has a minimum wear rate. But increasing the hardness of both wheel and rails will not secure better wear performance. Safety is also considered in this research using the derailment coefficient parameter. Based on the minimum derailment coefficient value among the combinations those with better wear performance showed a better safety.

Key words: wheel/ rail materials; hardness; material combination; wear rate.

Table of Contents

LIST OF FIGURES

LIST OF TABLES

NOMENCLATURE

AAR: Association of American Railroad

ASTM: American society for Testing and Materials

BHN: Brinell hardness number

EN: European standard

ORE: Office for Research and Experiments

RCF: Rolling contact fatigue

UIC: International Union of Railways

CHAPTER 1: INTRODUCTION

1.1 Background of the research study

Wear is a natural phenomenon that exists when two bodies, which are in contact, perform a relative motion; this is also true for the wheel and rail of a railway vehicle. This wear is mainly dependent on the type of material they are made of. There is a tolerable level of wear that is safe to the railway operation. Once this critical wear level is reached, it is mandatory to re-profile the wheel, grind the rail. However, after some time it will be worn out to the level it can no more be used and the whole system must be replaced with a new one.

All the above process demands a lot of time, human effort and costs large amount of money, so a small improvement on the wear rate reduction could have a great impact on such a large scale railway operation. There have been researches made to reduce the wear rate. One of the most effective approaches is to play on the material, as mentioned above the material in which the wheel is made of is different from the one in which the rail is made.

There are different lists of materials for the rail and for the wheel, which have been discovered by different researchers. All these materials are steel based but with different hardness and other mechanical properties. We can select or set new combination of materials like ER7 for the wheel and 60E1 for the rail. These materials are recently used in Europe [4]. The word ‘combination’, used in the above sentence is to indicate that a matching between a wheel made of ER7 steel and a rail made of 60E1steel material could be done for railway operation. The aim of this research is to set new combinations (pairs) of wheel and rail materials, test them for wear performance then compare the result with the existing ones and identify for the best material combination.

1.2 General overview on wear of wheel and rail materials

During train operation, the wheels of railway vehicles are subjected to wear. When the worn state of the profiles reaches a limit value defined by international standards, the wheels have to be re-profiled. In the railway community, it is well known that there are mission profiles (operation conditions, track geometry, wheel-rail profiles, etc.) where some train sets require the re-profiling of their wheel sets after only 80.000 km of service, whereas others are able to operate in similar conditions for more than 400.000 km without need such maintenance procedure. Furthermore, the railway wheels can only be re-profiled 3 or 4 times and the wheel set substitution is very expensive. The excessive wheel wear implies that, conversely, also the rails are subjected to premature deterioration. Thus, the complete characterization of the wheel wear problem allows tackling the rail wear problem as well [8].

According to the study of Deutsche Bahn (DB) systmtechnik [9]. Given the increase in traffic volumes over recent years, the service life of rails in the track and in switch systems is now determined less by wear-related attrition and increasingly by rolling contact fatigue that can lead to surface damage in the form of head checks and squats or, indeed, complete impairment of a rail's functional properties. Ever since high-speed services were introduced, therefore, an intensive search has been on for means of extending the service life of rails. One option is to use rail materials of greater strength that accordingly have a higher resistance to rolling contact fatigue (RCF). It is possible with pearlitic rail steels to either reduce the lamellar spacing in the pearlite through heat treatment (head-hardened rail), add alloying elements or raise the carbon content in the steel (hypereutectoid steels). All these measures lead to an increase in material strength and hence of resistance to wear and RCF. One alternative pursued in recent years is the use of bainitic rail steels. In conjunction with the appropriate alloying additions and, if need be, a suitable form of heat treatment, these can attain even greater strengths than pearlitic steels. Over recent years, DB Systemtechnik has been investigating the suitability of pearlitic and bainitic rail steels for use on lines with rolling contact fatigue problems with the aim of cutting track maintenance input without increasing the level of vehicle maintenance due to increased wheel wear.

By using pearlitic and bainitic rail steels to establish their suitability for use on track curves with rolling contact fatigue problems has shown that, as well as reducing wear, higher-strength pearlitic grades also result in shallower head checks, enabling them to at least delay the attendant damage done to the rail. The present findings indicate that, with suitable alloying and control of the form sulphides take, non-heat-treated, naturally hard steels could well be developed as an alternative to the head-hardened rail, especially since the wear at weld joints to which head hardened rails are subject would cease to exist.

Regardless of its lower sulphur content and its spheroidised sulphides, the R220 grade is unsuitable for lines with RCF problems, because its low yield strength encourages ratcheting and though level of wear is higher than that of the standard R260 grade, it does not suffice to prevent the propagation of head checks.

Bainitic rail steels allow a low-level balance between the processes of wear and rolling contact fatigue to be ensured. However, minimum strength values need to be observed when using them due to the altered wear mechanisms compared to pearlitic steels. The present findings indicate that high-chromium steels with a medium carbon content and hence of considerably greater strength deliver better wear behavior than high-manganese steels with low carbon content. The welding technique for these steels is more demanding and they are more expensive to buy, hence this is a type of steel that can only be recommended for lines where serious RCF problems necessitate considerable maintenance input.

With regard to the wheel/rail interaction, emphasis needs to be given to the finding that, in Amsler tests, the higher-strength pearlitic rail steels did not manifest a higher degree of wear than the two standard-wheel steels of differing strength tested. Conversely, the wheel steel of greater strength actually induced lower wear on the rail steel samples. This suggests that using higher strength steels for both wheels and rails impacts favorably on wear in the system as a whole in that it ensures more sustained profile stability.

According to Wolfgang Schoech study, harder and more wear resistant steel grades, such as the heat treated rail steel R350HT, are applied in curves up to 700 m radius on the high rails, which suffer from lateral wear and the low rails, which are affected by short wave corrugation. Furthermore this heat treated rail steel has proven in many track tests, that it

is not only more resistant against wear and corrugation compared to the standard rail steels, but also significantly more resistant against head checks.

The convincing technical and economic benefits of head hardened rails have been adopted by many infrastructure managers and led to the initiation of a step change in the policy on the use of rail grades of railways. Until now mixed traffic operators use mostly the two grades R260 and R350HT. Railways with increased axle loads, Heavy Haul railways in particular use high strength rail steels with hardness of 370BHN and above. These rail steels are now also in test with mixed traffic lines.

The European standard EN13674-1 has implemented in the year 2011 all available steel grades ranging from 200BHN (as-rolled) up to more than 400BHN (hyper-eutectoide, head hardened). Rail re-profiling has become today a common measure to maintain rails. It is accomplished by grinding, milling or paining. In the following, the term grinding is used for simplicity reasons.

Rail grinding has been implemented by many infrastructure managers by some means or other. Thereby it is still more addressing removal of longitudinal irregularities such as corrugation and to provide an optimized rail/wheel contact. RCF is treated in an increasing way by rail grinding, whereby generally more corrective actions are planned; occasionally a more strategic (preventive) approach is gaining ground. Soft rail steels wear and deform plastically quicker than harder rail steels, which require expensive corrective rail grinding and early rail renewal. Therefore these rails are more and more replaced by harder rail grades. However all pearlitic rail steels develop sooner or later RCF defects depending on the specific loading conditions.

Manufacturing industries like Amsted Rail [7], a leader in freight rail road industry for more than a century provide different railway materials. This company for instance uses the toughest wheel material which is Griffin's patented micro Alloy steel [7]. The wheel is tough enough with a 72% longer wheel life at heavy operation conditions. This indicated a 72% reduction in wheel set removals, lower operating expenses and less time for wheel maintenance.

According to the study of (Venkatarmi Reddy) [10] ,Australia in the years (2000-2004), have purchased approximately 500,000 tons of replacement rails per year at an estimated total cost of US $1.25 billion . Even a small improvement in rail performance has significant economic benefits to rail industry (Kristan, 2004). In 2000, the Hatfield accident in UK was caused due to rolling contact fatigue. It killed 4 people and injured 34 people and led to the cost of £ 733 million for repairs and compensation payments. In 1977, the Granville train disaster in Australia killed 83 people and injured 213 people. These accidents were mainly due to wear, rolling contact fatigue (RCF) and poor maintenance.

Rail wear and RCF are inevitable due to rail wheel interaction. These problems have increased the maintenance and replacement costs. If undetected, these problems can cause derailment causing huge loss of revenue, disruption of service, resulting damage of assets, and loss of lives. RCF alone costs European railways around € 300 million per year and these defects account for about 15% of the total costs. The total costs of all defects are about € 2 billion per year. The American Association of Railroads (AAR) estimated that the wear and friction occurring at the wheel/rail interface of trains due to ineffective lubrication, costs American Railways in excess of US $ 2 billion each year. The Office for Research and Experiments (ORE) of the International Union of Railways (UIC) has noted that maintenance costs increases directly (60–65 per cent) with increase in traffic, train speed and axle load. These costs are greater when the quality of the track is poor.

Multi-body simulation is today the most feasible method for the prediction of the safety, wear, fatigue and noise behavior of rail vehicles. A multi-body system is described by a limited number of interconnected rigid or flexible bodies. The behavior of the system is then obtained through analysis (e.g. time-integration) of the equations of motion: The multi-body software computes the dynamic movement of and the interactions between the different components of the train and of the track. An important aspect concerns the frictional interaction between wheels and rails. Because of computational efficiency, simplified models are generally used. Due to the rapid increase of computational power

and due to algorithmic speed-up as well, it is nowadays feasible to use more detailed rail-to-wheel contact models in vehicle system dynamics simulations as well.

SIMPACK Rail is an advanced multi-body package for the simulation of the dynamic running behavior of railway vehicle systems on the track. In order to achieve a calculation speed sufficient for dynamic simulations with actual vehicles, the rail-to-wheel contact locations and forces are determined by means of an approximate, non-iterative method, called equivalent-elastic. Its results are usually accurate enough for the daily work of vehicle manufacturers, engineering service providers and operators, i.e. predicting hunting, derailment and traction forces and providing the excitations needed for passenger comfort and component fatigue analyses [11].

Many laboratory techniques were used to find new steel types to get the optimum wear resistant materials for wheels and rails. Based on these studies fully pearlitic steels [3] (a mixture of ferrite and cementite) have been developed with yield strengths greater than 900Mpa and a good balance of mechanical properties. Similarly new wheel material have been tested and commercially produced as mentioned above.

According to the work conducted by Melbourne Research Laboratories [2], different rail types have different influence on the wear of wheels. This finding support greatly that a proper test should be performed while selecting the right wheel/rail material combination. Rail manufacturers nowadays sell improved materials which greatly exhibit higher strength and hardness properties. These improvements are achieved either by heat treatment or by addition of alloying elements. To test these improvements and to determine the wear behavior of wheel and rail materials under contact conditions, generally cylindrical specimens machined from actual rail and wheels are used. More sophisticated tests had also been used by using small diameter samples with scaled wheel and rail profiles. But the results of both experiments were limited and the researchers felt that the test technique should closely simulate the real life situation. This was because of the fact that wear occurs over the whole of the wheel/rail flange area. After this observation the Test Rig was designed and manufactured. For this research such

expensive test equipments are not used but a highly efficient modeling software SIMPACK will be used.

1.3 Problem statement

Different countries like China, America, India and German spend millions of dollars annually for repairing and replacement of worn wheels and rails, for instance America spent more than 900M dollars for wheel replacement in the year 2010-2011 and 32.2% of it is due to wheel wear[6].

Researches show that improved rail materials like the standard carbon steel grade R260 reduced wear rate significantly when it replaced the R200 half a century ago. Recently improved materials like AAR (Association of American Railroad) classes, AAR Class C, AAR Class B, and ER7 are widely used for the wheel and Thyssen/Krupp60E1 for the rail [5].The purpose of this research is to find a better material combination between wheel and rail for further reduction of wear rate, which in turn reduces a great amount of expense. For this research I will develop a model using SIMPAK software to simulate an actual wheel/rail interaction condition. Many researches like the one done by Roderik A Smith [1] focus on a new material for the wheel/rail and some others perform a test for the wear behavior based on real experimental setups. However, my research does not aim to find for new sets of materials, instead I will perform a matching between the existing wheel and rail materials and test for their wear behavior so that we can identify the effective combinations of wheel/rail materials with minimum wear rate.

1.4 Objectives of the study

1.4.1 General objective

This research will identify the best material combination between wheel and rail of a railway vehicle with minimum wear rate. The purpose is to find new sets of wheel and rail material combinations that could resist wear significantly.

1.4.2 Specific objective

This research will select combinations (matching) out of the recently used pairs of wheel and rail materials.

- The purpose is to take one standard wheel material and pair it with another standard of rail material. and run them together on a track.
- Select five pairs of wheel and rail materials as a combination
- Simulate them for their wear rate and derailment coefficient calculation using computer simulation (software) SIMPACK.
- Compute maximum wear rate
- Analyze the specific volume of material removed
- Compute derailment coefficient
- Compare the wear rate and the specific volume of material removed with the existing pairs.
- Identify for the best material combination in terms of minimum wear rate.
- In addition, derailment coefficient is compared between the combinations in order to check the safety.

1.5 Significance of the study

This study could provide wheel and rail material combination that have a longer life. The study on the other hands minimizes the frequency of failure, provides higher safety and saves a lot of maintenance and replacement cost for railway corporations and the country in general. The study may also provide new and competitive sets of material combinations for wheel and rail manufacturing companies.

The simulation model provides an easy ground for similar researches, wheel and rail material development and any wheel rail contact related studies. The model also saves a great amount of time, effort and money that is spent for organizing an actual laboratory experiment.

1.6 Scope of the study

This study tries to find the wear performance of five pairs of wheel and rail materials, create a SIMPACK model for the test and based on the result set a conclusion on which of the combinations is the best in terms of wear resistance and safety using the derailment coefficient value.

1.7 Limitations

For this research, it is not possible to perform actual laboratory tests because it is very expensive to get samples of all the materials to be tested. Since there is no wheel and rail manufacturing company in our country, equipments like the wheel/rail rig test used for experimentation are not available.

1.8 Outline of thesis report

This paper consists of six chapters. The first chapter deals with the introduction while the second chapter focuses on the review of literatures related to this paper. Chapter three addresses techniques and previously used results import to this paper .Chapter four comes with SIMPACK modeling and analysis, and chapter five deals with the results and discussion on the simulation outputs. The last chapter that is chapter six gives conclusion, recommendation and future work based on the results.

1.9 Research methodology

The methods used to do this research are the following:-

1. Data collection and study on recently used wheel/ rail materials.
2. Vehicle modeling and simulation using SIMPACK software.
3. Result analysis
4. Conclusion and recommendation

CHAPTER 2: LITERATURE REVIEW

2.1 wheel and rail wear

The contact that exists between the wheel and rail of railway vehicle causes damage on the wheel threads, flange and the surface of the rails. One point to note here is that the wheels are always in contact with the rail but the rail is free of contact once the vehicle passes. Due to this, the wheels become worn out before the rails.

The surface damages are the combined result of wear, plastic deformation, rolling contact fatigue and thermal fatigue.

Figure 1: Wheel / rail contact

Figure 2: Wheel thread wear [21] **Figure 3: Rail wear [21]**

2.2 Standard wheel and rail materials

2.2.1 Wheel grades

The materials employed in wheels and rails in Europe are steels whose predominantly pearlitic structures containing hard cementite having high resistance to wear. According to UIC Leaflet 812-3 (table 1) for solid wheels lists seven types of steel, which mainly differ in carbon content, heat treatment state and therefore strength, and EN 13262 contains only four types (Table 1). Grade R1 for freight wagon wheels is becoming less favorable than the standard R7 material, and Grades R2/R3 has never been used in operational practice. R7 is the most commonly used grade. It is used for all freight wagon wheels and on most passenger vehicles. Where wheels made from R7 are intended for use in vehicles with tread brakes. Experience has shown that where carbon content exceeds 0.5%, the K_{IC} values of 80MPa $\sqrt{m}$ can only be attained where comparatively small grain size (fine grain), high purity and high homogeneity are present in the microstructure throughout the circumference of the wheel. This places heavy demands on manufacturing quality. For this reason, these wheels are commonly supplied with lower carbon contents (<0.5%C) which puts them often in the lower strength tolerance range, so that besides pearlite, large amounts of pre-eutectoid ferrite are present in the tread.

Although this leads to greater toughness, the wear resistance is correspondingly diminished. According to Deutsche Bahn's (DB)experience, a free (pre-eutectoid) ferrite content of≤10% is advantageous in terms of minimizing wheel wear at the tread. For driven wheels on locomotives and motor coaches, R8 is increasingly the used grade. In summary, materials employed for solid wheels in Europe are largely restricted to unalloyed steels with maximum carbon content of 0.56% and – after appropriate heat treatment (fine pearlitization) of the tread – tensile strengths of at least 820 to 980MPa in maximum[21].

2.2.2 Rail grades

At 0.6 – 0.8%, the carbon content of the European standard Grade 900A rail is higher than that of the wheel materials. However, its maximum tensile strength is 1050N/mm², as this grade of rail is used in its naturally hard condition, i.e. without subsequent fine pearlitization. Heat treatment of the railhead is generally an option. Rails of this type are described as "head-hardened" and, to minimize wear in the outer rail, are generally used only on track where the curve radius is <700m.

Table 1: Wheel steel requirements according to UIC 812-3 and EN 13262 [21]

Steel category		Carbon content	Yield strength	Tensile strength	Elongation (%)	Notch impact energy (J)	
UIC 812-3	EN13262	UIC/EN	EN 13262	UIC/EN	UIC/EN	UIC 812-3	UIC 812-3
R1 N	-	≤ 0.48	-	600-720	≥ 18	≥ 15	-
R2 N	-	≤ 0.58	-	700-840	≥ 14	≥ 10	-
R3 N	-	≤ 0.70	-	800-940	≥ 10	≥ 10	-
R6 T, E	ER6	≤ 0.48	≥ 500	780-900	≥ 15	≥ 15	≥ 12
R7 T, E	ER7	≤ 0.52	≥ 520	820-940	≥ 14	≥ 15	≥ 10
R8 T, E	ER8	≤ 0.56	≥ 540	860-980	≥ 13	≥ 15	≥ 10
R9 T, E	ER9	≤ 0.60	≥ 580	900-1050	≥ 12	≥ 10	≥ 8

N, normalized T, heat treated E, whole wheel heat treated

2.3 Material composition in relation to wheel rail contact

The contact resistance b/n wheel and rail is proportional to the length of the contact patch and, hence, resistance is minimized if, for a given geometry, the contact area is kept small by choosing materials with a high elastic modulus. Of the common and inexpensive metals, steel has one of the highest values of elastic modulus. For this reason and because steel is relatively inexpensive and have a very good combination of strength, ductility, and wear resistance almost all wheels and rails worldwide are made from plain carbon-manganese pearlitic steel, which has a lamellar structure of iron and iron carbide. Table 2 Illustrates typical wheel and rail chemistries and hardness values. In general, passenger vehicle wheels tend to have lower carbon content and hardness than heavy axle load freight vehicles. Steel of about 300Brinell hardness is typically used for rail in straight track, while rail in the hardness range 340 to 390.

Table 2: Typical Chemistry and Hardness of Freight and Passenger Wheels and Rails [27]

		C (wt %)	Mn (wt %)	S (wt %)	P (wt %)	Hardness (Brinell)
Rail	Standard	0.75	0.90	0.02	0.02	290
	Hardened	0.75	0.90	0.02	0.02	370
Passenger wheels	Standard	0.50	0.80	0.04 max	0.04 max	260
	Hardened	0.55	0.80	0.04 max	0.04 max	270
Freight wheels	Standard	0.62	0.72	0.05 max	0.05 max	300
	Hardened	0.72	0.72	0.05 max	0.05 max	340

2.4Mechanical and chemical processes used to obtain different grades

2.4.1 Hardness and chemical composition

Either the Association of American Railroads (AAR) or the American society for Testing and Materials (ASTM) specifications (M-107 and A 504-49, respectively) dictate the manufacturing of steel wheels. The specifications outline five wheel classes (U,L,A,B and C) and serve as guidelines for intended service conditions, steel carbon content and heat treatment (table 3.). All wheel steels contain between 0.060 and 0.85 weight percent (w%) Mn, less than 0.05 w% each of s and p and more than 0.15 w% Si. Class L, A,B and C wheels are rim quenched and tempered to meet required hardness.

Table 3: Carbon content in weight percent, the Brinell hardness number (BHN in kg/mm^2) and intended service condition for steel wheel classes [25]

Class	W % C	BHN	Service Condition
U	0.65-0.77	____	General service where an untreated wheel is satisfactory
L	≤0.47	197-277	Light wheel loads, high speed service, more severe braking conditions than other classes
A	0.47-0.57	255-321	Moderate wheel loads, high speed service, service braking conditions
B	0.57-0.67	277-341	Heavy wheel loads, high speed service, severe braking conditions
C	0.67-0.77	321-363	(1) High wheel loads under light braking (2) Heavier braking conditions employing off- tread brakes.

Wheels with class Asprting as S plate design. Production of steel wheels is as follows. Wheel blocks are heated to 1175^0F , descaled with high pressure water jets and upset forged into a disk. A rough wheel rolling contours the wheel tread, flange, rim faces and plate while maintaining the desired diameter. The wheel is then coned and the hub punched followed by controlled cooling to 1000^0F. At this point class U wheels are slowly cooled to 300^0F. The remaining classes are reheated to 1600^0F for heat treatment. Submersion in water quenches only the rim. Hardness requirements , rim thickness and wheel diameter dictate quench times. Reheating to 900^0F tempers the quench. The final forging step is slow cooling to 300^0F. Final dimensions are achieved by turning on a lathe followed by inspection of surfaces, dimensions, concentricity, internal quality , plate shot peening and final inspection.

Rim quench and temper practices increase the wear resistance of the tread surface and produce a residual compressive hoop stress. Because the AAR and ASTM specifications mandate only a single Brinell hardness measurement as the target for successful heat treatments, variation between wheels and manufacturers can be expected.

2.4.2The effect of carbon content

The higher the carbon content, the higher the wear resistance. However higher carbon content tends to increase thermal damage.

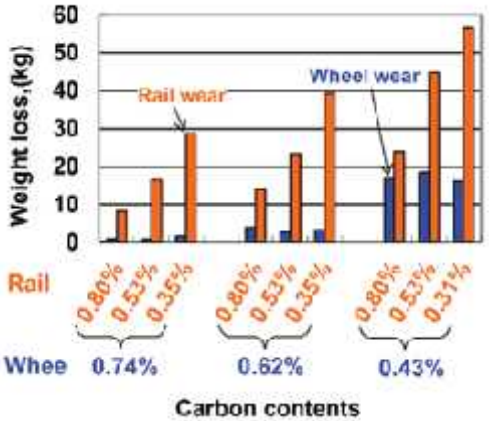

Figure 4: Carbon content Vs Wear [26]

Symbol	E				ρ
value	$210*10^{9}$ N/m^2	$2060*10^{-8}$ m^4	0.3	$66.3*10^{-4}$ m^2	7850kg/m^3

Table 4: Typical Mechanical properties of UIC 50 rail steel [28]

2.5 Wear reduction method

2.5.1 Grinding

RCF defects are sites at which transverse cracks are relatively likely to initiate and thence to propagate, leading to broken rails. The decarburized surface material of new rails is relatively easily damaged and may be subject to rapid wear. Plastic flow can give rise to undesirable interaction between wheel and rail, decreasing the running stability of the vehicle, and can, in addition, be a direct cause of defects. Short- and long-pitch corrugations can cause track irregularity and deterioration of track components, and give rise to noise and ground vibration. Removal of these rail defects contributes to the cost of railway maintenance. Failure to remove these defects is even more costly to railroad corporations.

Regular rail grinding is one of the most effective and widely accepted measures for minimizing such rail defects.

CHAPTER 3: WEAR ANALYSIS TECHNIQUES AND PREVIOUS RESULTS

3.1 Rig testing

According to the Deutsche Bahn (DB) wheel-rail system test rig, rolling contact between wheel and rail is simulated at full-scale. It is a wheel on roller test rig (Fig. 4). The full-size wheelset under investigation rolls on a driven rail roller consisting of two rail tyres measuring approx. 2100mm in diameter formed from standard 900A grade rail steel. The profiles of both the wheels and the rail tyres correspond to DB's normal matched wear profiles. The wheelset is mounted on a single-axle auxiliary rotary frame and can be loaded with axle loads of up to 30 tons at speeds of up to 300km/h. Curving conditions with contact of the gauge corner at an adjustable angle of attack, also like straight track conditions, can be controlled dynamically. Loadings scenarios must approach the loads imposed on the wheelset during vehicle service as closely as possible. They are based on the vehicle parameters and a combination of travel through curves and in a straight line, varying speeds, braking maneuvers and weathering conditions. In order to achieve reproducible results within short test time frames, critical service conditions such as tight curves and emergency braking were emphasized out of normal proportion.

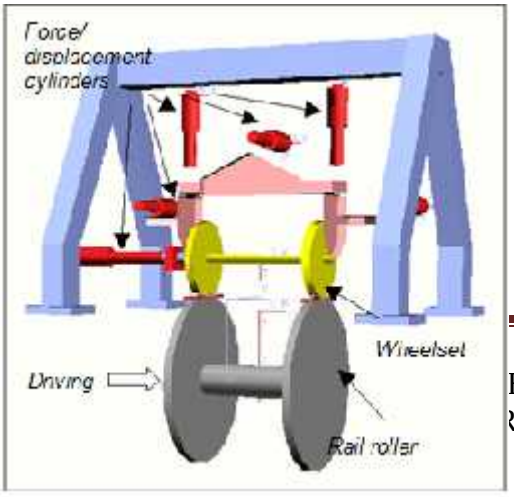

Figure 5: Wheel-rail test rig, schematic [21]

3.2 Wear analysis results from previous researches using the test rig

Comparison of Shinkansen material with R7

Test conditions:

- Mean axle load: 13 tons

- Straight ahead and curving with radii R = 600 to 1,800m

- Speed: 110 - 190km/h

- No rail lubrication

- End of test run if lateral force >30kN and bearing acceleration >250m/s² as the limit for wheel out of roundness

- Wheels were re-profiled between the first and second tests

Results:

It was found that the development of wheel out of roundness is heavily dependent on the material. In the first test run, the wheels made of Shinkansen steel already managed two and a half times the running performance of the R7 wheels before the appearance of comparable out of roundness.

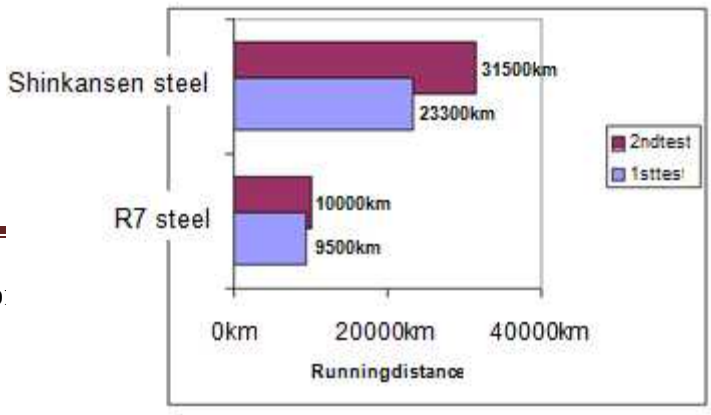

Figure 6: Running distances for getting wheels out of roundness

After the wheels had been re-profiled to a depth of approx. 2.5mm, the second test run with the Shinkansen steel wheels was terminated after 31,500km, even though the limit values for lateral force and bearing acceleration had not been reached compared to R7 wheels. This confirmed the expectation that the steel with the higher carbon content and strength level exhibits a better wear behavior and that wheel out of roundness can be considerably delayed. One reason for this appears to lie in the absence of free ferrite from the wheel tread. After the test, only the R7 wheels showed small rolling contact fatigue cracks in the tread ("Treadchecks").

In parallel with the wheel investigation, changes in profile to the head of the rails were recorded and evaluated. In this way the potential for heavier damage to track due to the new wheel material can be identified and assessed in a timely manner. The wear ratio of the wheel and rail was determined before and after the test from the cross-section of the wheel tread and rail head and the ratio of the circumferences of the wheel and rail tyres. This coefficient indicates the ratio in which wheel and rail material are "consumed" on each rolling revolution, i.e. the extent to which a harder wheel causes greater wear on the rail, and vice versa. Accordingly, a ratio of 1 means that the wheel and the rail wear to a similar extent. In the previous case, a wheel-rail wear ratio of 0.86 was determined for the Shinkansen steel. In other words, there is a slight tendency for wear to be transferred more to the rail. It is not possible to make a conclusive assessment at present for the wheelset fitted with R7 wheels because this value was subject to far greater variability. Further test rig investigations should create clarity on this point.

3.3 Wear analysis results from previous researches computer simulation

A review of a wide range of research and published papers and test results has shown that there is no basis to conclude that an increase in material hardness on one side of the wheel/rail interface will result in an increase in wear rate on the opposite side of the interface. No evidence has been found to support the notion that the total 'system' wear rate is constant. In addition,

Many researchers have observed that an increase in hardness on one side of the interface can actually be beneficial in reducing wear on the opposite side.

Different wheel/rail wear literatures [12] reviewed that the belief that an increase in the hardness of the rail, while giving a decrease in the rail wear rate, will give an increase in wheel wear is not generally felt to be justified". This conclusion was based on a review of a large number of studies from different organizations and researchers in the UK and abroad.

Laboratory twin-disc tests conducted on pearlitic rail steels by BR from 1981 [13] showed that the wear rate of the wheel steel was practically independent of the steel against which it was run for a wide range of load conditions (covering both the mild and severe wear regimes). Graphs of the total 'system' wear showed that this dropped as the rail hardness increased. BR also undertook tests on a full-size wheel/rail rig [14] which found that both rail and wheel wear were reduced as the rail hardness was increased. Similar effects were reported in a large number of research papers, for example [15, 16]. Although not all the papers described a reduction in wheel wear with increasing rail hardness, they all showed a reduction in total system wear and none reported an increase in wheel wear.

It was suggested that the reduction in wheel wear with high strength rails may be associated with a reduction in the surface deformation damage on both the wheel and rail samples: the reduced volume of wear debris from the harder

rail material resulted in less abrasive wear occurring on the wheel material. Some tests (for example, [17]) found that increasing rail hardness resulted in a clear tendency for wheel wear to decrease. In summary, the review of laboratory wheel/rail wear tests

[12]concluded that the wear of one component is either unaffected or is decreased by changes in hardness of the other. The actual effect is dependent on the metallurgy (which affects the nature of the wear debris produced) of the harder component, but a reduction in wear debris volume (due to the increased hardness) might be expected to be less abrasive to the softer material.

More recently, a series of tests were undertaken by DB Systemtechnik [18] to determine the effect of increasing rail hardness (to resist RCF) on wear of both the wheel and rail. A series of laboratory and track tests were undertaken to test these rail materials, but due to the relatively short sections of rail being tested it was not possible to determine the effect of the rail materials on wheel wear from the track tests. In the laboratory tests no significant difference in wheel wear was obtained for any of the rail steels tested, apart from a head hardened material, for which a drop in the wheel wear rate was obtained. They concluded that higher strength steels for both wheels and rails had a favorable impact on wear of the system as a whole and helped sustain profile stability.

One of the work streams in the InnoTrack project undertook twin-disc tests on premium grade rail steels to test their RCF resistance [19]. During the tests wear of the wheel material was also measured. The tests were undertaken in both dry and wet conditions. The results showed no clear relationship between rail hardness and wheel wear under dry contact conditions but a drop in wheel wear rate for an increase in hardness when ‘wet’. They also observed that increasing the rail hardness did clearly show a significant drop in total system wear under all contact conditions.

Wear of either wheel or rail material is a result of a combination of i) the forces generated in the contact patch and ii) the response of the material to those forces. If the material on one side of the contact patch is made more wear resistant, then its own characteristic material response to wheel/rail forces has changed. However, if the wheel/rail profiles are the same then the location of the contact point between wheel and rail, and the total force,

which needs to be transmitted, will be the same, irrespective of the rail material hardness. The wheel material will therefore be required to transmit the same force through essentially the same contact patch area (changes in rail material hardness may affect the size of the contact patch due to plastic deformation, but these changes will mostly be small and most of the contact force is transmitted through the center of the contact patch) and its own wear rate is driven by the forces it needs to transmit: the material on the opposite side of the contact patch will see no significant change in the contact forces and does not 'know 'what the hardness of the other material is. Therefore it should not be expected for the hardness of one material to have an effect on the response of the other material. The only exception to this, and this was discussed in some of the research papers, would be if the change in material properties were to change the nature of the wear debris, causing more debris to become entrained in the contact patch, making the contact conditions more severe, and increasing wear by abrasion. This may be the reason for some materials having a bigger impact on the wear rate of the other material than others. However, when the rail material hardness is increased then the lower wear rate will produce less wear debris, so it might be expected that the wheel material wear rate would also go down. Therefore, it should not be a surprise that increasing the hardness of the material on one side of the contact patch should help reduce the wear rate on the other.

Other considerations in contrast to the test results it could be possible for the wear rate of wheels to increase in the presence of harder rails if the rail (or wheel) profile is not optimal, resulting in more severe contact forces. With normal grade rail a more aggressive contact condition would cause the wear rates of both the wheel and rail to increase, for a short time, until the profiles had become more 'conformal' and more 'friendly'. However, a rail with a more wear-resistant characteristic would retain its 'unfriendly' shape for longer, causing increased wheel/rail forces and more wheel wear before it wore to a better shape. Therefore, in the presence of harder grade rails it is important to ensure that rail profiles are managed and maintained to control the contact forces better.

A review of a wide range of research and published papers and test results has shown that there is no basis to conclude that an increase in material hardness on one side of the wheel/rail interface will result in an increase in wear rate on the opposite side of the interface. No evidence has been found to support the notion that the total ‘system’ wear rate is constant. In addition, many researchers have observed that an increase in hardness on one side of the interface can actually be beneficial in reducing wear on the opposite side.

3.4 Wear parameters and mathematical analysis

3.4.1 Forces at the Contact Patch

Within the wheel/rail contact patch, a force exists normal to the plane of the contact, mainly due to the load (weight) of the wheel on the rail. In addition, tractions are produced in the plane of contact by the vehicle steering forces. This force system produces complex hydrostatic and shear stresses in the rail and wheel. Of most interest is the compressive contact stress normal to the plane of contact, which has a generally elliptical distribution and affects both wheel/rail wear and rolling contact fatigue. The maximum value of the contact stress p_o, occurs at the center of the ellipse, and is given by:

$$P_o = \left(\frac{6P E^{*2}}{\pi^3 R_e^2}\right)^{1/3} \left[F\left({R'}/{R''}\right)\right]^{-2/3} \quad \ldots\ldots\ldots\ldots\ldots\ldots\ldots (1)$$

where P is the normal load, E^* depends on the wheel and rail elastic moduli, $F(R'/R'')$ is a function of the wheel and rail radii of curvature, and Re is the equivalent relative curvature of the wheel/rail system, defined as $Re = (R'R'')^{1/2}$.

3.4.2 Creep

Pure rolling rarely takes place, and wheels and rails are not rigid. The normal load between wheel and rail causes local elastic deformation and an area of contact, the contact patch, is formed. In the case where the surfaces of the wheels and rails are smooth

and have constant curvature in the location of the contact patch, the contact patch is elliptical in shape, and the distribution of normal pressure between wheel and rail over the contact patch is semi-ellipsoidal.

If a longitudinal force is applied to the wheel, so that it is braked, a deviation from the pure rolling motion occurs. The deviation in relative velocity divided by the forward speed of the wheel is referred to as the longitudinal creepage. Similarly, lateral creepage is defined as the (incremental) relative lateral velocity divided by the forward speed. In addition, relative angular motion between wheel and rail about the normal to the contact patch is referred to as spin. If the longitudinal creepage is small, it is accommodated by elastics trains in the location of the contact patch. As the wheel rotates, unstrained material enters the contact patch at its leading edge. As the material moves through the contact patch, the relative velocity between the wheel and rail equals the rate of change of strain so that the surfaces are locked together. The magnitude of the resulting longitudinal tangential stress increases linearly with distance from the leading edge. Similarly, lateral creepage gives rise to lateral tangential stresses. Both longitudinal and lateral creepage therefore generate forces which are directly proportional to the corresponding creepage.

Creep is a natural consequence of having fixed wheels on a solid axle, and is defined with respect to the forward and lateral wheel and rail velocities:

$$Longitudinal\ creep(s_n) = 2\left(\frac{V_R^F - V_W^F}{V_R^F - V_W^F}\right) \ldots\ldots\ldots\ldots\ldots\ldots\ldots\ldots\ldots\ldots (2)$$

$$Lateral\ creep(s_y) = 2\left(\frac{V_R^L - V_W^L}{V_R^F - V_W^F}\right) \ldots\ldots\ldots\ldots\ldots\ldots\ldots\ldots\ldots\ldots (3)$$

Where V refers to velocity; subscripts R and W refer to the wheel and rail, respectively; and superscripts F and L refer to the forward and lateral directions. There is a further type of creep, known as spin creep, which is caused by a relative rotation of the wheel and rail around an axis normal to the plane of contact. This type of creep (Equation 4.) is also implicated in wheel and rail damage.

$$Spincreep(s_y) = 2\left(\frac{\Omega_R - \Omega_W}{V_R^F - V_W^F}\right) \qquad (4)$$

In general, a wheelset will always be moving laterally with respect to the rail (producing lateral creepat each contact patch), and each wheel will not be moving at the forward speed of the vehicle (thereby producing longitudinal creep at each contact patch). All three types of creep will usually be present, although one may dominate.

Thus, the steering force on a wheel saturates at a value equal to the wheel load times the adhesion coefficient. This saturation occurs at a resultant creep of about 0.01. Relationships between these three types of creep and the resultant forces and moments have been derived by Kalker.

The steering forces caused by creep lead to surface and near-surface shear stresses that produce deformation in the contact patch. This deformation increases rolling resistance, and, more importantly, contributes to increased wear and rolling contact fatigue.

3.4.3 Evaluation of the contact forces

The calculation of the contact forces for each contact point is based on a semi-elastic approach which uses both Hertz's and Kalker's global theories. The normal contact force, according to Hertz's theory, depends both on the penetration p_n between the surface of wheel and the rail and on the penetration velocity $v_n = V * n_r^r(P_r^{rC})$, where **v** is the contact point velocity,

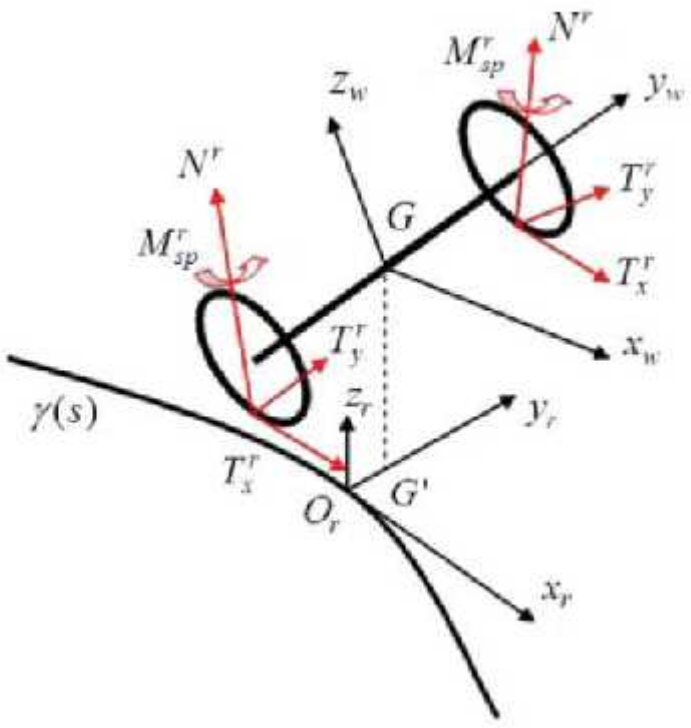

Figure 7: The nomenclature of the contact forces [22]

Assuming that it is rigidly connected to the wheel:

$$N^r\left(P_r^{rC}\right) = \left[-k_h[p_n]^\gamma + k_v[v_n]\frac{sgn(v_n)-1}{2}\right]\frac{sgn(p_n)-1}{2} \quad \ldots\ldots\ldots\ldots\ldots\ldots\ldots\ldots (5)$$

Where γ is equal to 3/2, k_h is Kalker's stiffness constant depending on the surface geometries and the material properties and k_v is a damping contact constant. The same theory also allows to evaluate the contact patch semi axes *a*, *b* and the ellipse eccentricity. Linear Kalker's theory is then applied to calculate the tangential forces and the spin moment(Figure 6) in each contact patch:

$$T_x^\tau\left(P_r^{r,C}\right) = -f_{11}\xi_{x'}$$

$$\begin{aligned} T_x^\tau\left(P_r^{r,C}\right) &= -f_{22}\xi_y - f_{23}\xi_{sp}, M_{Sp}^\tau\left(P_r^{r,C}\right) \\ &= -f_{23}\xi_y \\ &\quad - f_{33}\xi_{sp} \quad \ldots\ldots\ldots\ldots\ldots\ldots\ldots\ldots\ldots\ldots\ldots\ldots\ldots\ldots\ldots\ldots\ldots\ldots\ldots\ldots (6) \end{aligned}$$

where the value of the f_{ij} coefficients, which are the functions of the material properties and

the ellipse semi axis. ξ_x, ξ_y and ξ_{sp} are the longitudinal, lateral

and the spin creepages, as defined below:

$$\xi_x = \frac{V * i_r}{\left\|\dot{G}^r_{W.f}\right\|};\quad \xi_y = \frac{V * t^r_r}{\left\|\dot{G}^r_{W.f}\right\|};\quad \xi_{sp} = \frac{\omega^r * n^r_r}{\left\|\dot{G}^r_{W.f}\right\|}, \qquad (7)$$

Where $\dot{G}^r_{W.f}$is the absolute velocity of the wheelsetcentre of mass, i_r is the unit vector of the x_r axis, ω_r is the wheelset angular velocity expressed in the auxiliary reference system and$t^r_r = n^r_r \times i_r$. Since Kalker's theory is linear, to include the effect of the adhesion limit due to friction, a saturation criterion has to be introduced in the model to limit the magnitude of the tangential contact force $\tilde{T}^r = \sqrt{\tilde{T}^{r2}_x + \tilde{T}^{r2}_y}$, which cannot exceed the slip value$T^r_z = \mu N^r$. Therefore,a saturation coefficient ε(Equation 8) is defined according to the Shen–Hedrick–Elkins formulation:

$$\varepsilon = \begin{cases} \dfrac{\mu N^r}{\tilde{T}^r}\left[\left(\dfrac{\tilde{T}^r}{\mu N^r}\right) - \dfrac{1}{3}\left(\dfrac{\tilde{T}^r}{\mu N^r}\right)^2 + \dfrac{1}{27}\left(\dfrac{\tilde{T}^r}{\mu N^r}\right)^3\right] & if\ \tilde{T}^r \le 3\mu N^r, \\ \dfrac{\mu N^r}{\tilde{T}^r} & if\ \tilde{T}^r \le 3\mu N^r, \end{cases} \qquad (8)$$

in this way, the saturated tangential force will be$T^r = \varepsilon T^r$.

3.5 The wear evaluation

3.5.1 The local contact model

The local contact model starts from the global contact variables evaluated by the vehicle

model (contact point positions, contact forces and spin moments, global creepages and patch semi axes) and calculates the local contact variables (normal pressures, tangential stresses and creepages) within each contact patch. The model is based on an approximate but very efficient version of Kalker's local theory implemented in his FASTSIM algorithm, commonly used in railway multibody simulations. The algorithm works in a local reference system, whose origin is situated at the center of the elliptical contact path, with the *x* and *y* axes defined in the common tangent plane to the contact surfaces, as shown in Figure 7; therefore, they are not parallel to either the local reference system of the wheelset or the auxiliary system.

The working hypothesis on which the algorithm is developed is the proportionality between the tangential pressure $\mathbf{p}_t$ and the elastic displacement **u** in a generic point of the contact patch:

$$\boldsymbol{u}(x,y) = Lp_t(x,y), \qquad L = L(\xi, a, b, G, v)$$

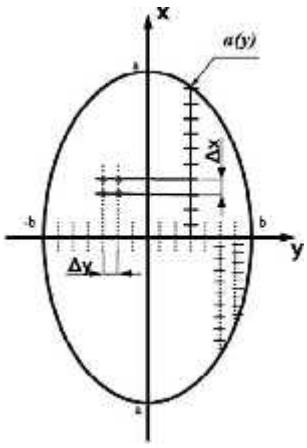

Figure 8: The contact patch discretization in the FASTSIM algorithm [22]

where the flexibility *L* is a function of the global creepage vector **ξ**, the ellipse semi axes *a*, *b*, the combined shear modulus *G* and the combined Poisson's coefficient *v*, as expressed below:

$$L = \frac{|\xi_x|L_1 + |\xi_y|L_2 + C|\xi_{sp}|L_3}{\sqrt{\xi_x^2 + \xi_y^2 + C^2\xi_{SP}^2}} \quad \ldots\ldots\ldots\ldots\ldots\ldots\ldots\ldots\ldots\ldots\ldots\ldots\ldots\ldots(9)$$

in which $L_1 = {}^{8a}/_{(3G_{c11})}$, $L_2 = {}^{8a}/_{(3G_{c22})}$, $L_3 = {}^{8a}/_{(3G_{c23})}$ and $c = \sqrt{ab}$.

Kalker's parameters c_{ij}, which are functions of *a/b* and *v*, can be easily found from table. The local creepages in a generic point can be obtained by deriving the elastic displacements and considering both the rigid global creepages and the vehicle speed *V*:

$$o(x,y) = u(x,y) + V\begin{bmatrix}\xi_x \\ \xi_y\end{bmatrix} \ldots\ldots\ldots\ldots\ldots\ldots\ldots\ldots\ldots\ldots\ldots\ldots\ldots\ldots(10)$$

The calculation of the local variables p_n, $p_t$and $\boldsymbol{\sigma}$ is performed in each point of the grid adopted tomesh the contact patch (Figure 7): the transversal axis of the contact ellipse, with respectto the travelling direction, is divided into $n_y - 1$ parts with a length of

$$\Delta y = {}^{2b}/_{(n_y - 1)}$$

by means of $n_y$equidistant nodes. Similarly, the longitudinal sections of the patch which are$2a(y) = 2a\sqrt{1-(y/b)^2}$long are divided into $n_x - 1$ equal parts of

$\Delta x(y) = 2a(y)/(n_x - 1)$ length using n_x equidistant nodes. This choice leads to a non-constant longitudinal resolution which increases nearby the lateral edges of the ellipse, where the length *a(y)* is shorter. So, the accuracy near the edge is appreciably higher than that obtainable with a constant resolution grid that would produce more numerical errors. The n_x and n_y parameters have to be chosen as a compromise between numerical efficiency and precision; the range 25 ÷ 50 has proven to work fine. The expressions of the normal pressure and the adhesion limit pressure in a generic point(x_h, y_l) of the grid, with $1 \le h \le n_x$, $1 \le l \le n_y$, are as follows:

$$P_n(x_h, y_l) = \frac{3}{2}\frac{N^r}{2\pi ab}\sqrt{1 - \frac{x_h^2}{a^2} - \frac{y_l^2}{b^2}} \quad \ldots\ldots\ldots\ldots\ldots\ldots\ldots\ldots\ldots(11)$$

$$P_A(x_h,y_l) = P_t(x_h - \Delta x(yl), yl) - \begin{bmatrix}\xi_x \\ \xi_y\end{bmatrix}\frac{\Delta x(yl)}{L} = P_t(x_h - 1, yl) - \begin{bmatrix}\xi_x \\ \xi_y\end{bmatrix}\frac{\Delta x(yl)}{L} \quad \ldots\ldots(12)$$

Where N^r is the normal contact force. Starting from the values of the local variables in $(x_h-1,\ yl)$,the algorithm works iteratively to find the exact distribution of the local variables in (x_h, yl):

$$\|P_A(x_h,yl)\| \le \mu P_n(x_h,yl) \Rightarrow P_t(x_h,yl), \qquad \sigma(x_h,yl) = 0 \ldots\ldots\ldots\ldots\ldots\ldots\ldots(13)$$

$$\|P_A(x_h,yl)\| > \mu P_n(x_h,yl) \Rightarrow \begin{cases} P_t(x_h,yl) = \mu P_n(x_h,yl) P_A/\|P_A(x_h,yl)\| \\ \sigma(x_h,yl) = \dfrac{LV}{\Delta x(yl)}\left(P_t(x_h,yl) - P_A(x_h,yl)\right), \end{cases} \ldots\ldots\ldots(14)$$

where the boundary conditions are $p_t(x1, yl) = 0$, $\sigma(x_1, yl) = 0$, $1 \le l \le ny$, since creepages and pressures have to be zero outside the contact patch. Finally, the distributions of the pressures *pn (xh, yl)* and p_t *(xh, yl)* and the creepages $\boldsymbol{\sigma}(x_h, yl)$ are found by iterating the procedure for$2 \le h \le nx$ and $1 \le l \le ny$.

3.5.2 The wear model

As stated previously, the calculation of the wear on the wheel is based on an experimental law according to which the volume of the removed material correlates with the total frictional work. The main output of the wear model is the specific volume $\delta P_{ki}^{j}(t)(x,y)$, expressed in$mm^3/(mm^2m)$, a function of time which describes the specific volume (the volume per unit of area and per unit of travelled distance) of the material to be removed in the grid position(x, y) of the contact patch $P_{ki}^{j}(t)$.

The integral with respect to *x* and *y* over the grid gives the specific volume of the removed material per unit of travelled distance relative to the contact patch *Pjki (t)*. In fact, the subscript *Pjki (t)* indicates the contact patch i^{th} of the wheel j^{th} in the k^{th} multibody simulation of the statistical analysis of the track. With regard to the statistical approach, the track and its features will be explained in the next section.

The three indexes are variable in the following intervals:

• $1 \le j \le NW$, where NW is the number of wheels of the vehicle,

• $1 \le i \le NP$, where NP is the maximum allowed number of contact points (as will be explained below), and

• $1 \le k \le NC$, with NC being equal to the number of multibody simulations in the statistical description of the real track.

The quantity $\delta P_{kl}^{j}(t)(x,y)$ has to be evaluated in each point *(xh, yl)* of the contact patch grid.

To this end, the local frictional power in these points can be estimated by means of the *wear index* I_W (N/mm2*)*:

$$I_W = \frac{P_z * v}{V} \quad \text{(15)}$$

which is experimentally related (Figure 10) to the *wear rate* K(μg/m·mm^2): the wear rate gives a measure of the amount of material removed per meter of travelled distance (m) travelled by the train and per mm^2 of surface. The analytical expression for K (I_W) is given by Equation (16).

$$K_w(I_w) = \begin{cases} 5.3 * I_w, & I_w < 10.4\ N/mm^2 \\ 55.0, & 10.4 \le I_w \le 77.2\ N/mm^2 \\ 61.9 * I_w - 4723, & I_w > 77.2\ N/mm^2 \end{cases} \quad \text{(16)}$$

Normally, the wear rate on the tread is typically $K1$, while on the flange both the $K1$ and $K2$regimes occur. In this regard, Figures 11 and 12 shows an example of the frequency distribution of the two wear regimes along the lateral coordinate of the mean wheel profile (after taking the average on wheels and simulations)

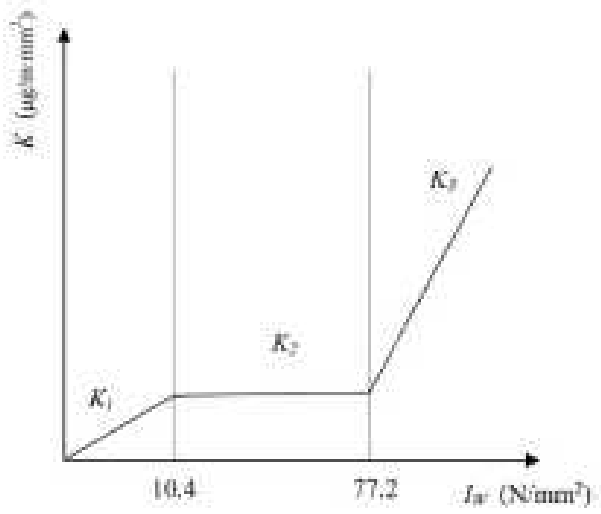

Figure 9: The wear rate as a function of wear index [22]

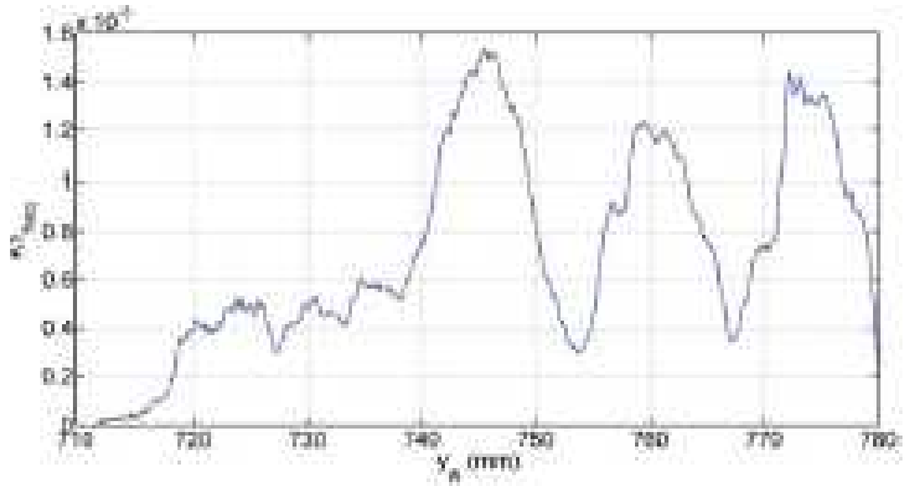

Figure 10: Typical frequency distribution of the K1 wear regime after taking the average on wheels and simulations [22]

After evaluating the wear rate, the specific volume $\delta P^{j}_{kt}(t)(x,y)$ can be calculated as follows:

$$\delta P^{j}_{kt}(t)(x,y) = \frac{K\, I_W}{\rho}\left(\frac{mm^3}{m\; mm^2}\right) \quad \ldots\ldots (17)$$

Where, ρ is the material density of the wheel and rail (expressed in kg/m^3).

CHAPTER 4: MODELING AND ANALYSIS

4.1 Vehicle modeling using SIMPACK

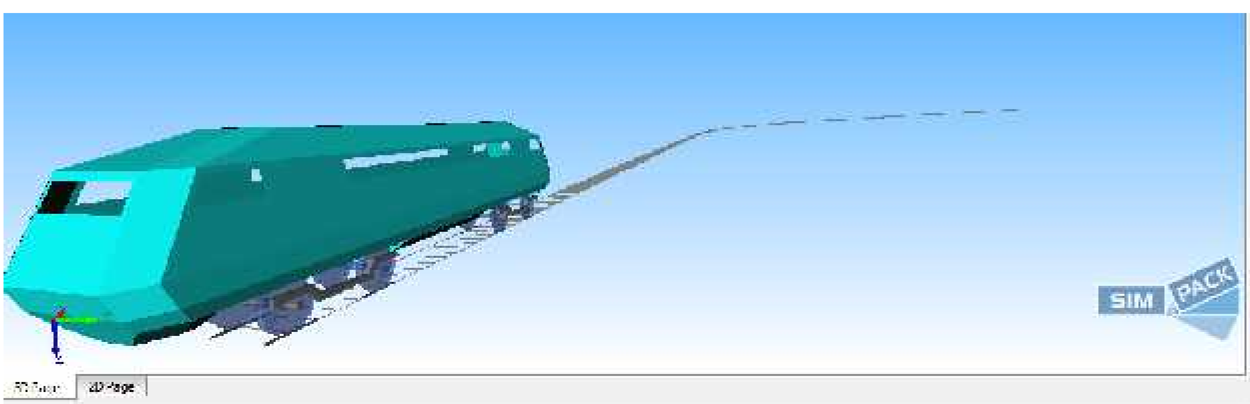

Figure 11: Vehicle model

4.1.1 Major Technique Parameters based on Addis Ababa LRT specifications [24]

1. Tramcar Width: 2650mm
2. Tramcar Height: 3700mm
3. Track Gauge: 1435 mm
4. Minimal Curve Radius: 50m for mainline and 30m for parking garage
5. Minimal Vertical Curve Radius: 1000m
6. Tramcar Length: 28400 mm
7. Wheel Base: 1900 mm for power bogie and 1600 mm for driven bogie
8. Wheel radius = 600mm
9. Axle load = 25ton
10. Maximum operation speed = 70 km/hr

4.1.2 Wheelset model

Steps used for the modeling of the wheel set

Step 1. Setting up the wheel set body

- Axle diameter 180mm
- Axle length 2200mm
- Wheelset 1000kg, Inertia mass I_{xx}= I_{zz}= 1000 kgm^2, I_{yy}=100kgm^2 , including the axle boxes

4.1.3 Wheel –Rail pair properties

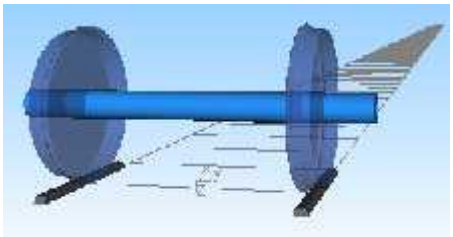

Figure 12: Wheel rail pairs

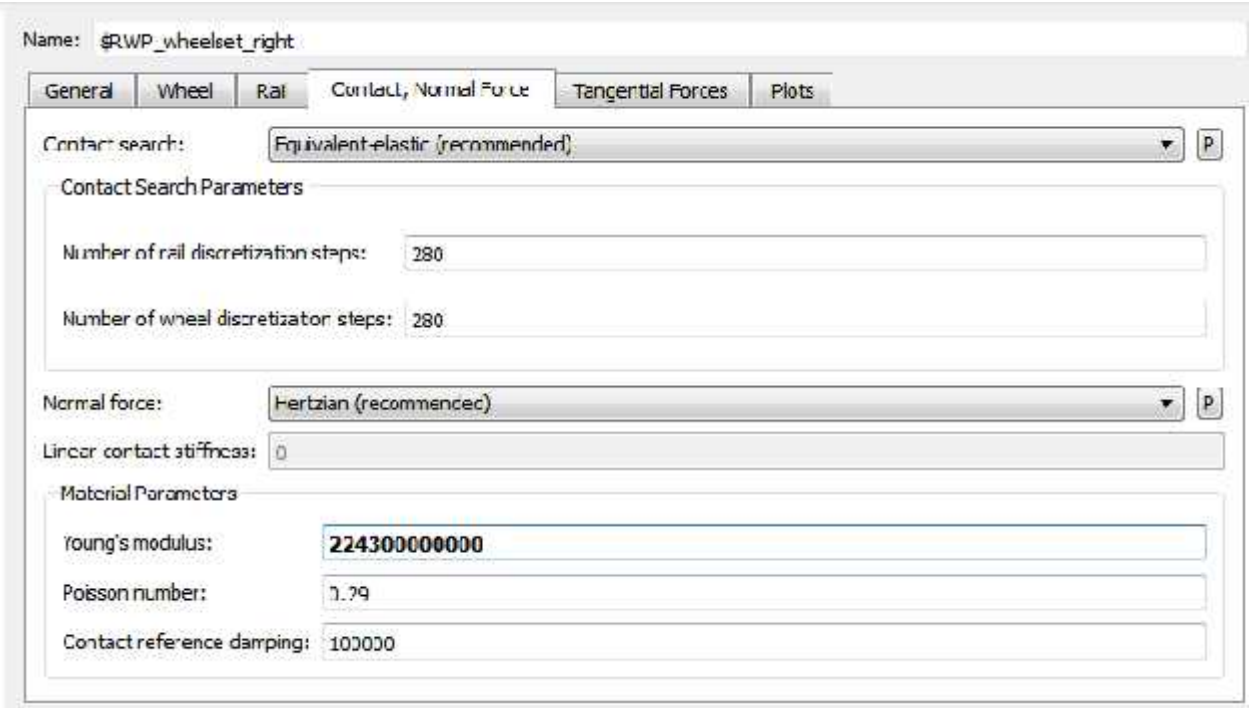

Figure 13: Young's modulus and Poisson's ratio (material combination 0)

`

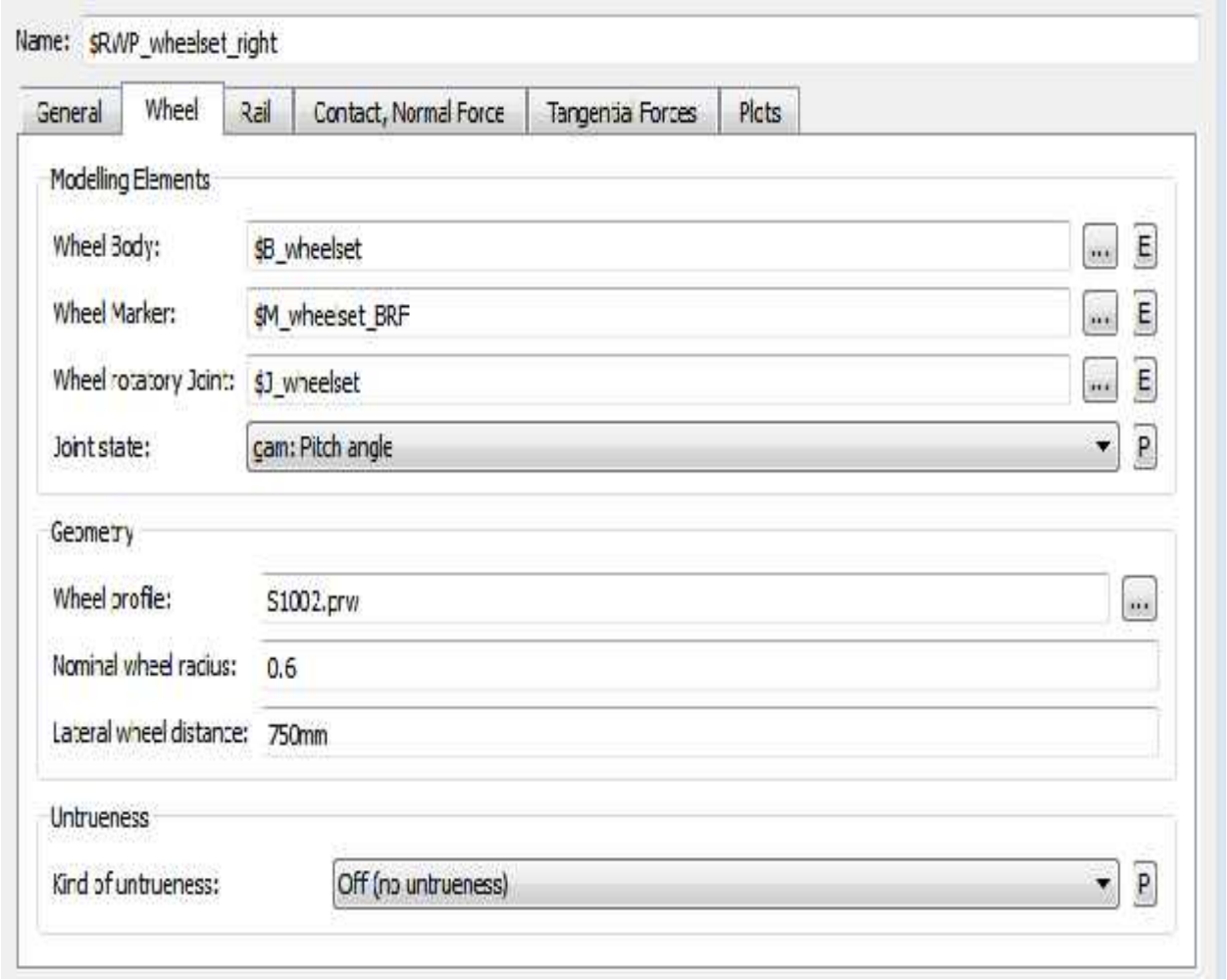

Figure 14: Wheel &Rail properties

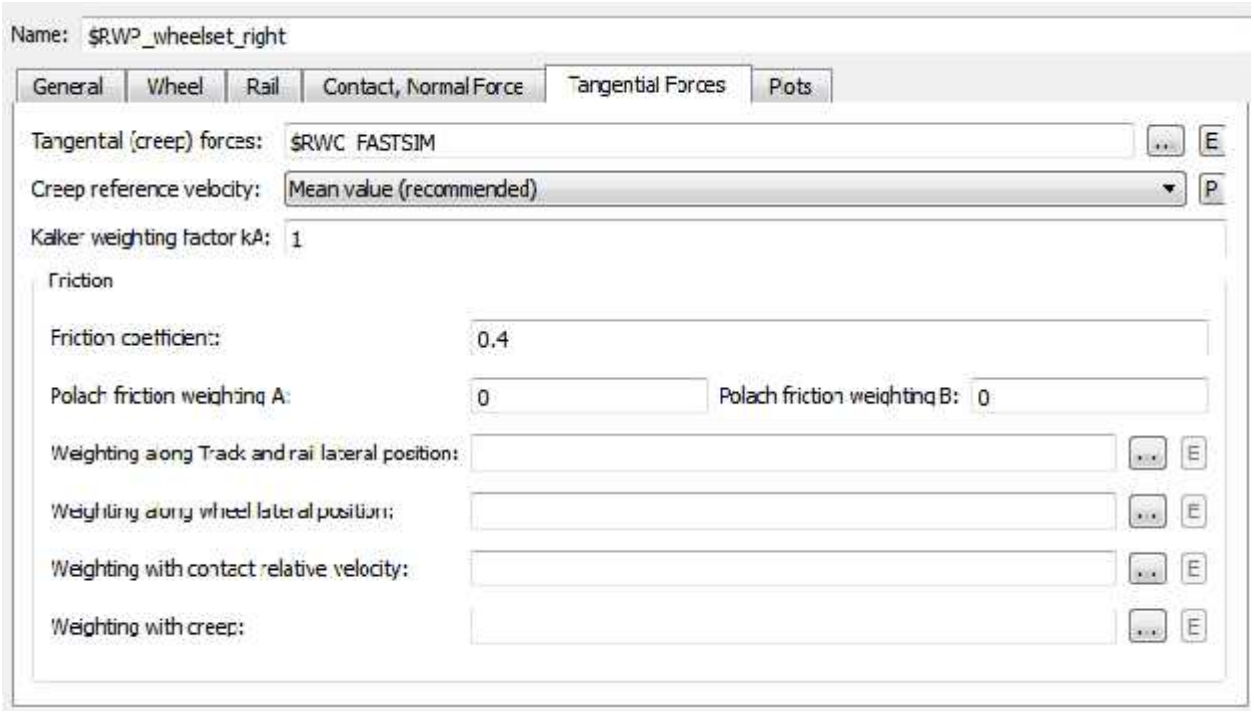

Figure 15: Coefficient of friction

- **Contact positions of the wheel-rail pair**

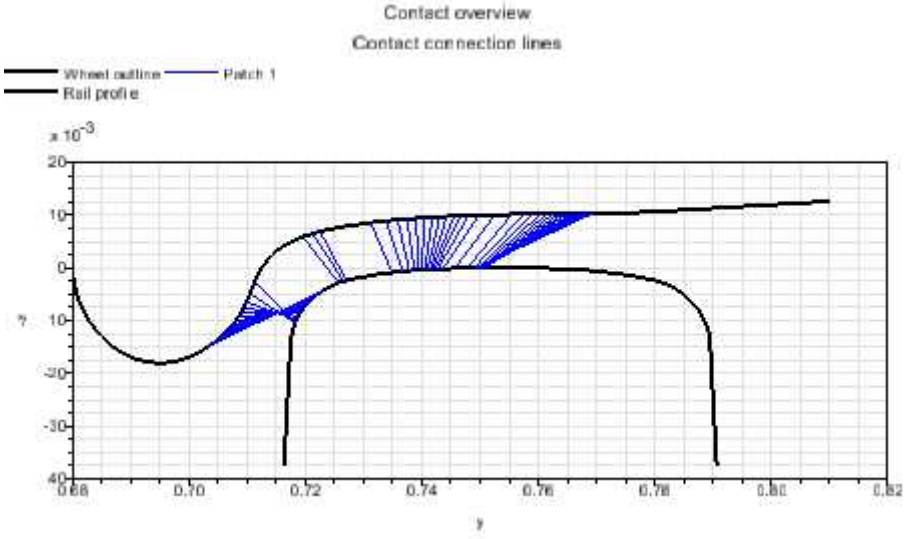

Figure 16: Possible contact region

- **Stiffness and Damping**

. The stiffness and damping values used are: cx = cy= 10 kN/mm (10^7N/m), cz= 5kN/mm ($5*10^5$N/m), and dx = dy= dz= 20 kNs/m ($2* 10^5$Ns/m).

. Create a *Force Element* of type 5

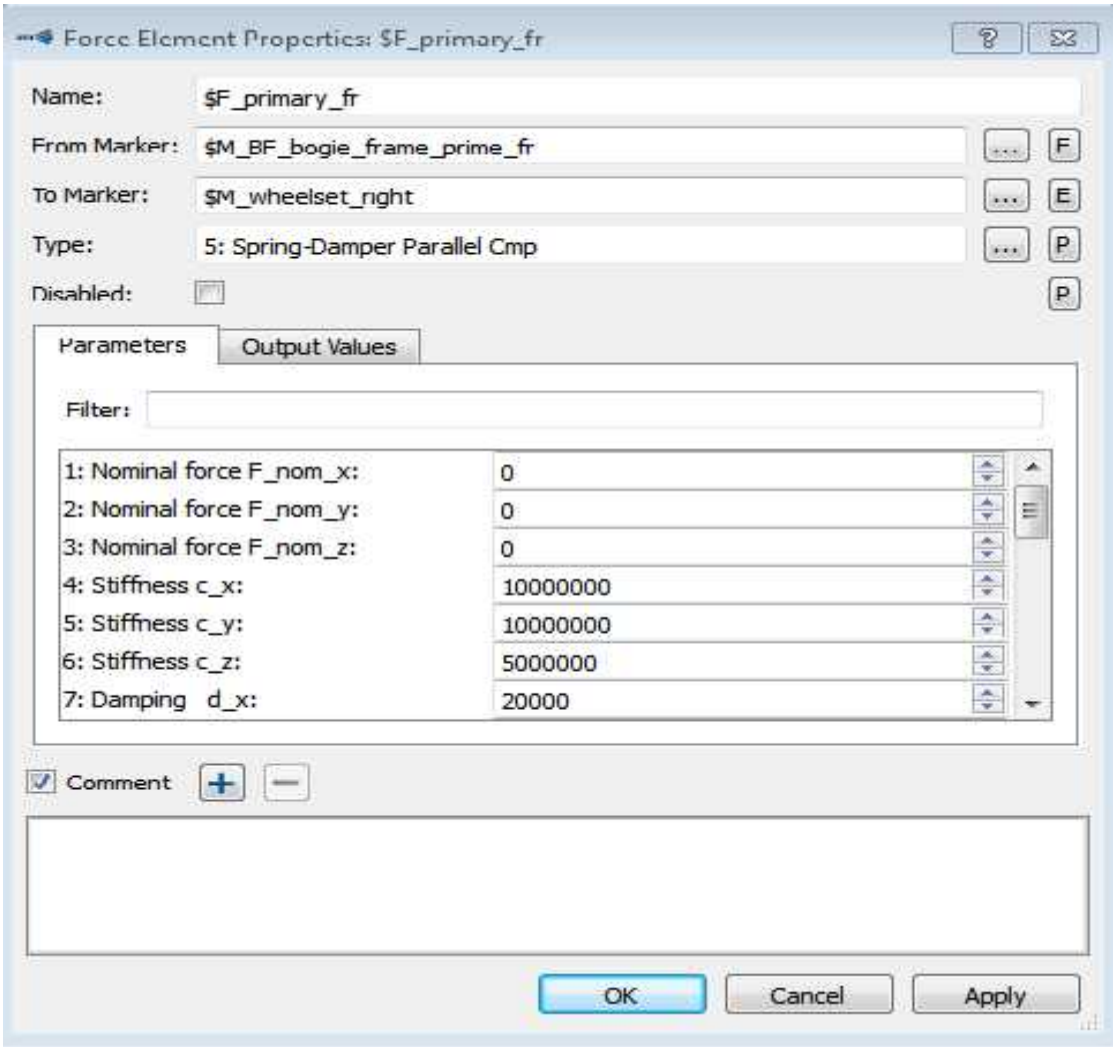

Figure 17: Primary suspension stiffness and damping values

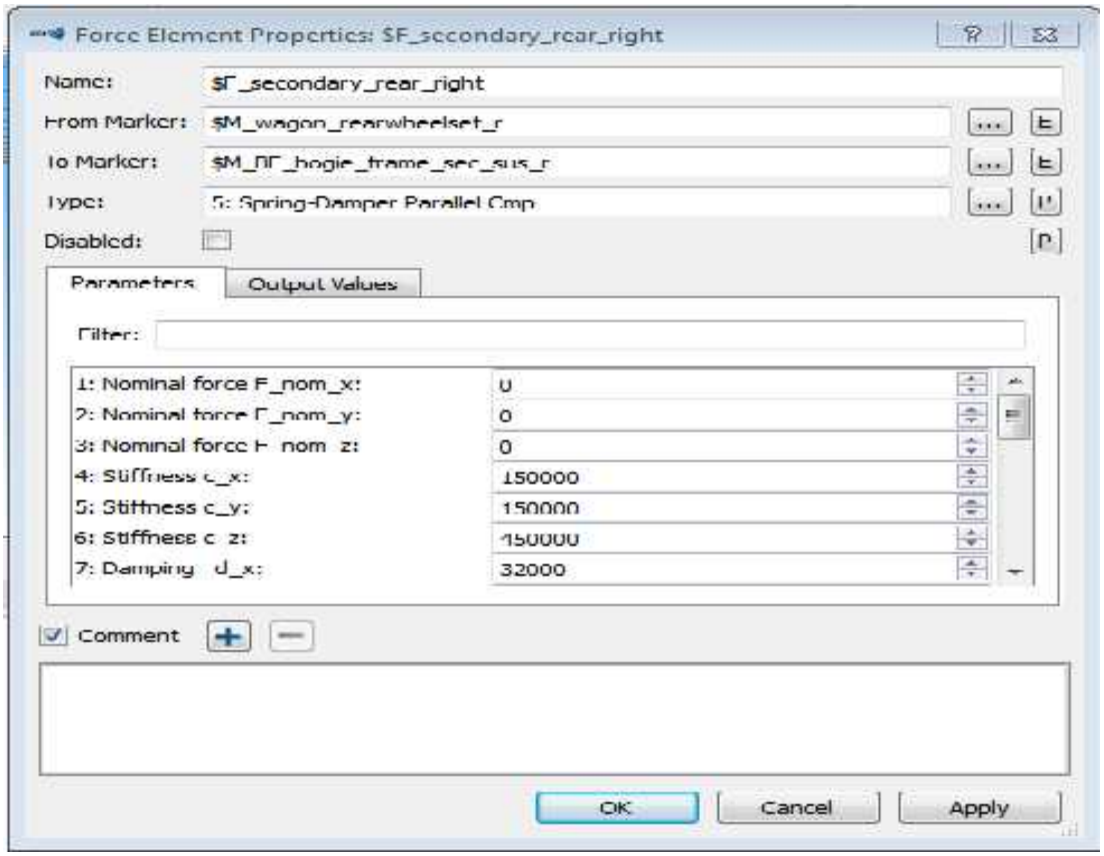

Figure 18: Secondary suspension

- **Vertical Load**

The same Force Element also exerts the vertical load.

. Create a *SubVar*'$_PS_Fz' with a value of, -50 kN. The minus sign is important because the force direction is related to the Force Element's From Marker: The guidance *Marker* must be 'pulled' upwards, in negative z direction, in order to have the wheel set

pressed on the rails.

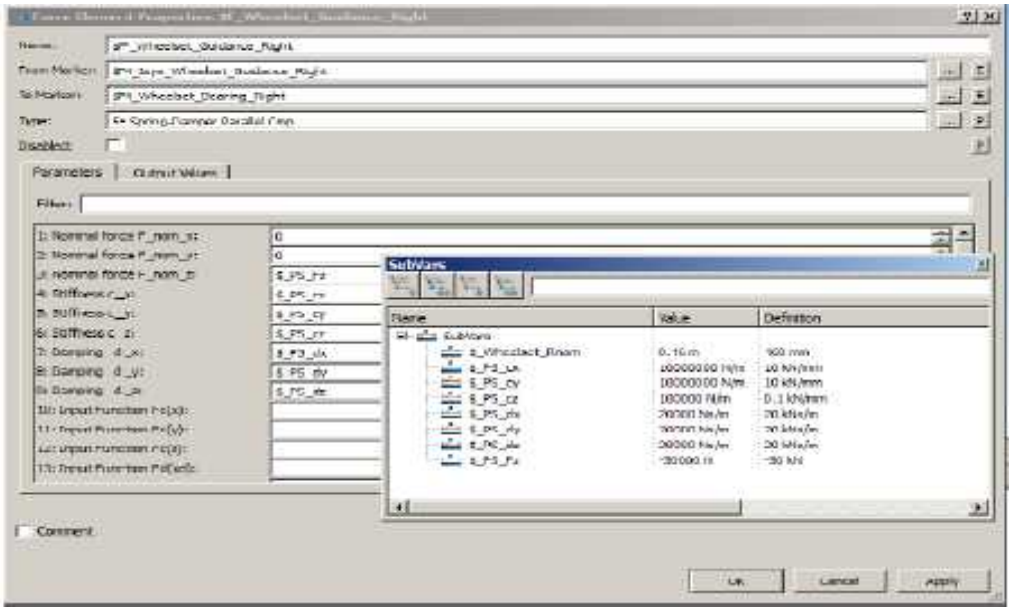

Figure 19: Markers and parameters of the guidance Force Element

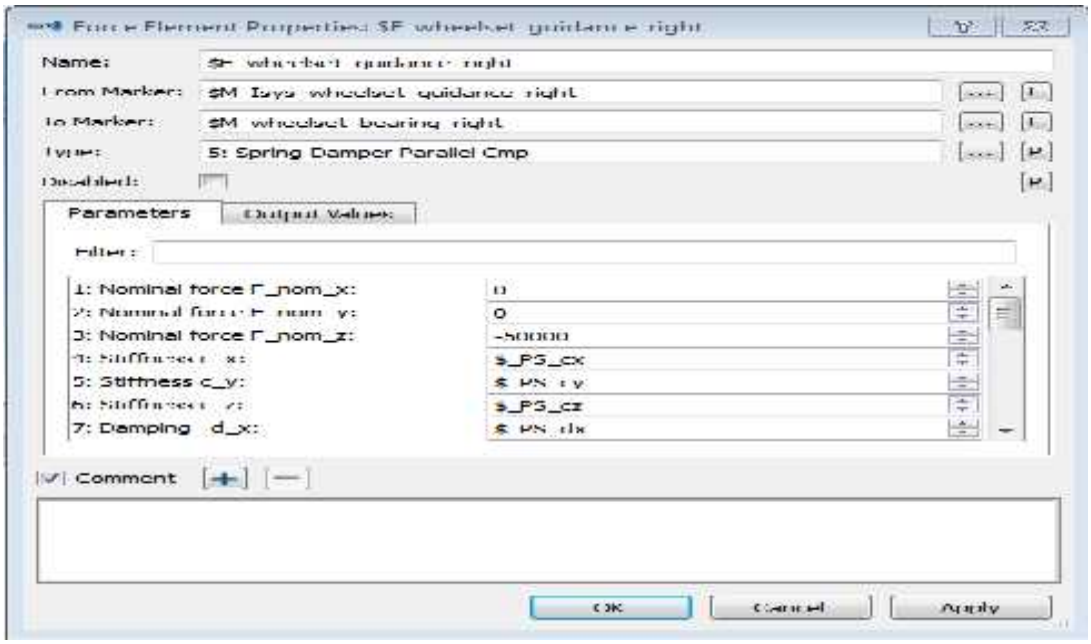

Figure 20: Application of the wheelset guidance force

4.1.3 Bogie model

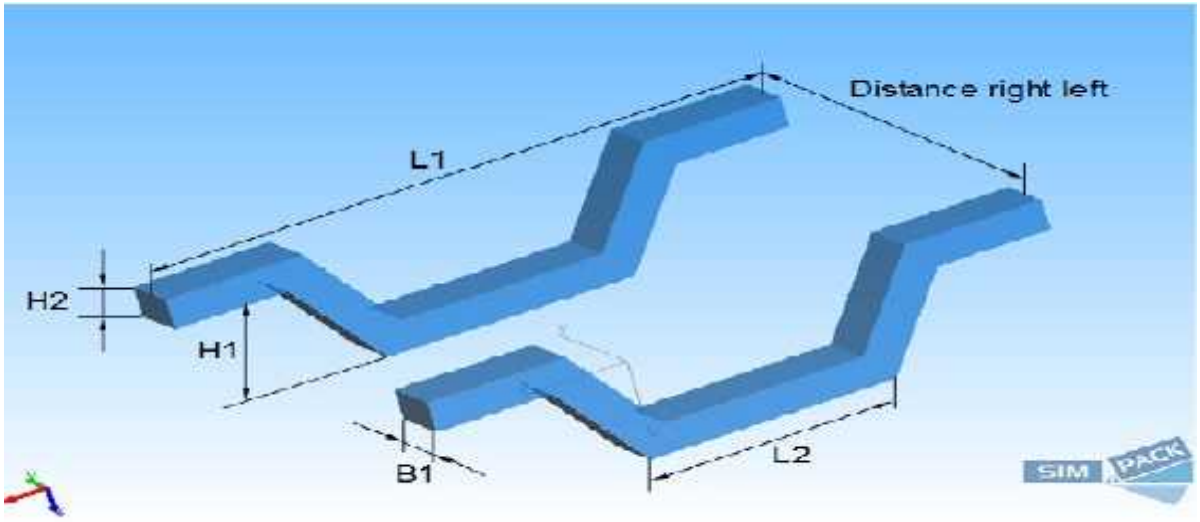

Figure 21: Bogie dimensions

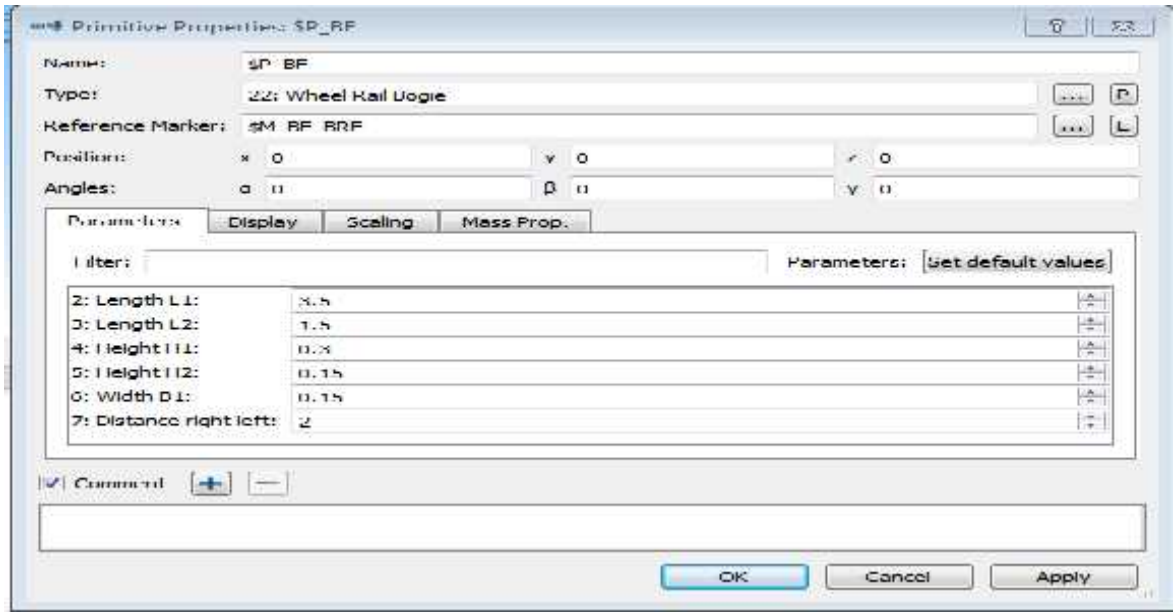

Figure 22: Bogie dimension inputs

4.1.4 Car body model

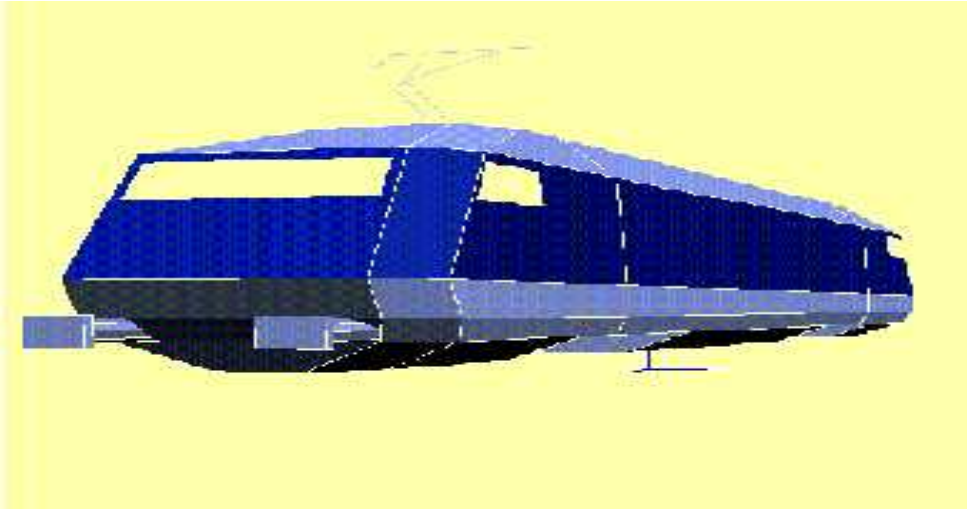

Figure 23: Car body [29]

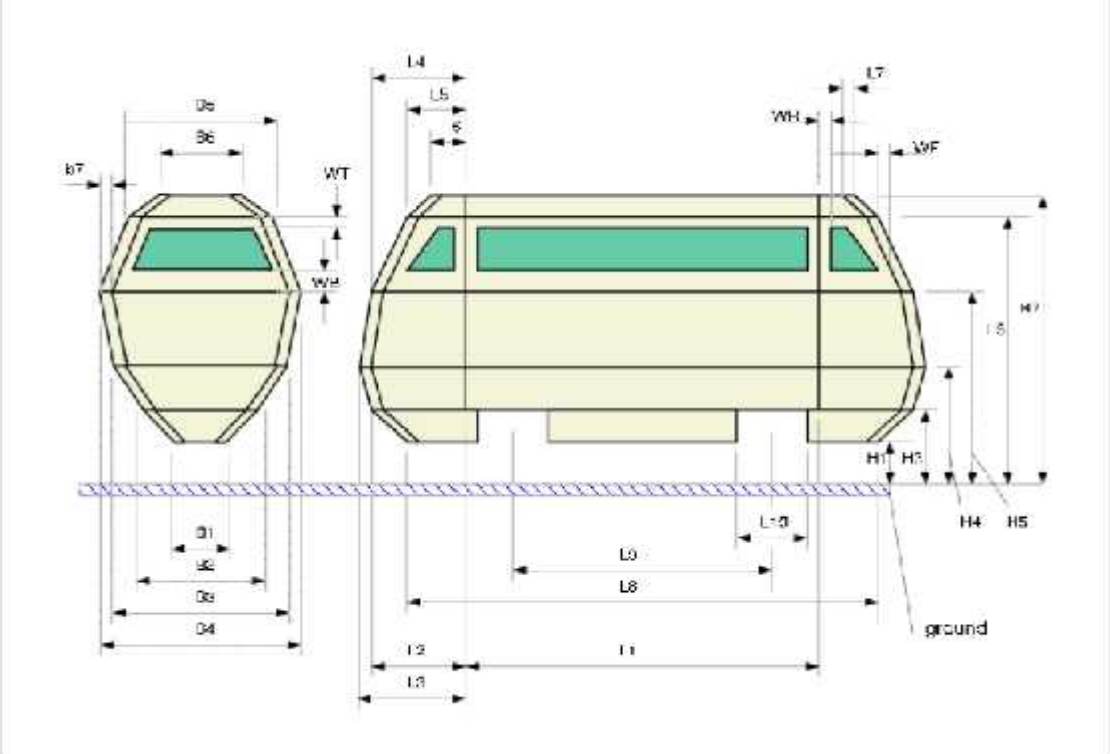

Figure 24: Car body dimensions [29]

In SIMPACK software primitive properties are used to denote the wagon dimensions which is presented in the figure below.

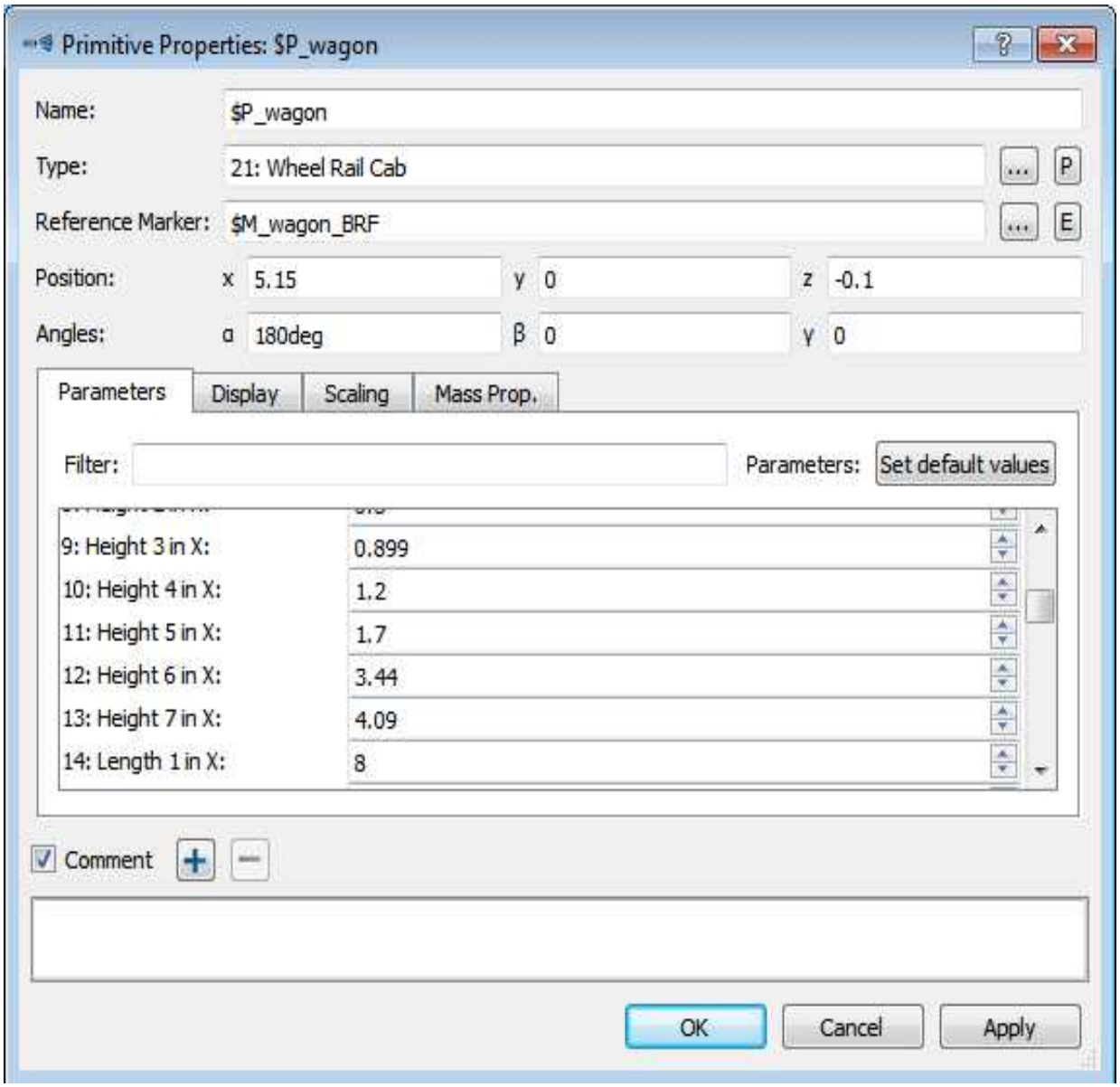

Figure 25: Wagon dimension inputs

4.2 Wear analysis and results

For the test I used four new combinations of wheel and rail materials and one material combination with similar property with the Addis Ababa LRT specifications (Material combination 0), the material combinations used for this wear analysis are presented as below.

4.2.1 Explanation on material combination

To make the concept material combination it is enough to see fig. 26 material combination implies simply a selection and matching of different standard of rail and wheels. It has no connection with mixing the materials of the wheel and rail chemically.

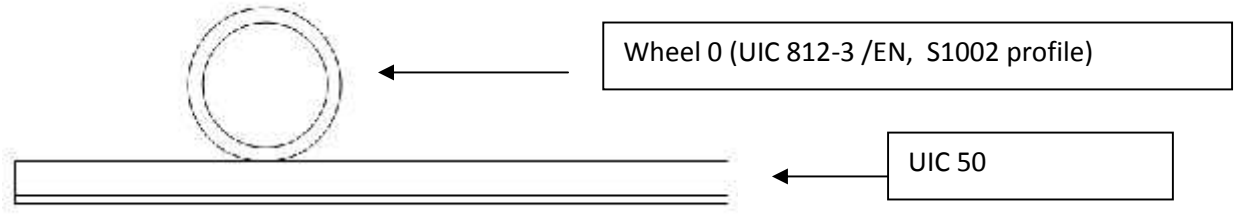

Figure 26: Explanation of Material combination, example: - Material combination 0

4.2.2 Heat treatment of the five material combinations

Table 5: Heat treatment of the selected materials

Combination	Wheel	Rail
Material combination 0	Normalized	Normalized
Material combination 1	Normalized	Normalized
Material combination 2	Whole heat treated (hard)	Whole heat treated (hard)
Material combination 3	Rim heat treated (hard)	Whole heat treated (very hard)
Material combination 4	Normalized	Whole heat treated (very hard)

4.2.3 Chemical composition and hardness of the five material combinations

Table 6: Chemical composition and hardness

Material combination		Chemical composition %					Hardness (BHN)
		C	Si	Mn	p	S	
Material combiantion0	Wheel	0.4	0.35	0.8	≤ 0.05	≤0.05	200
	Rail	0.6	0.5	1.3	≤0.05	≤0.05	240
Material combiantion1	Wheel	0.4	0.3	0.8	≤ 0.05	≤ 0.05	220
	Rail	0.6	0.1	1.3	≤ 0.04	≤ 0.04	260
Material combiantion2	Wheel	0.5	0.1	1.3	≤ 0.025	≤ 0.025	240
	Rail	0.6	0.1	1.3	≤ 0.03	≤ 0.03	270
Material combiantion3	Wheel	0.6	0.1	1.3	≤ 0.04	≤ 0.04	260
	Rail	0.8	0.1	0.8	≤ 0.025	≤ 0.03	350
Material combiantion4	Wheel	0.6	0.35	0.8	≤ 0.05	≤ 0.05	200
	Rail	0.8	0.1	0.8	≤ 0.03	≤ 0.03	350

4.2.4 Material properties and important inputs for the SIMPACK vehicle model

Table 7: Selected wheel/rail grades and their properties

Materials		Kg/m	Cross-sectional area (cm^2)	Tensile strength (Mpa)	Strain (elongation) %	E (Mpa)	Density Kg/m^3	Poissons ratio
Material combination 0	Wheel 0 (UIC 812-3 /EN, S1002 profile)			550	18	206	7800	0.29
	Rail 0 (UIC 50)	50	69.34	552	18	210	7210	0.29
Material combination 1	Wheel1(UIC 812-3 /EN, R7T,E S1002 profile)			545	18	206	7800	0.285
	Rail1 (UIC 60)	60	76.86	550	18	210	7806	0.285
Material combination 2	Wheel2 (UIC 812-3 /EN, R7T,E)			600	18	210	7850	0.28
	Rail2 (Chinese national railways, GB 2585-81)	50	77.65	880	10	210	7726	0.28
Material combination 3	Wheel3 (UIC 812-3 /EN,R9 T,E, S1002 profile)			550	16	206	7850	0.27
	Rail3Rail1 (UIC 60)	60	76.86	1050	16	210	7806	0.27
Material combination 4	Wheel 0 (UIC 812-3 /EN, S1002 profile)			550	18	206	7800	0.29
	Rail3Rail1 (UIC 60)	60	76.86	1050	16	210	7806	0.27

4.2.5 Input for the SIMPACK model

- **The combined young's modulus [29]**

$$E^* = \frac{2E_iE_j}{(1-v_i^2)E_j + (1-v_j^2).E_i} \quad \dots (18)$$

where,

E_i is the young's modulus of material i.

$E_j$is the young's modulus of material j.

$v_i$is the poisson's ratio of material I .

$$E_0{}^* = \frac{2*206*210}{(1-0.29^2)*206+(1-0.28^2)*210}$$

$v_j$is the poisson's ratio of material j.

Table 8: Combined young's modulus

Material combination	Combined young's modulus (Gpa)
Material combination 0	224.3
Material combination 1	228.55
Material combination 2	229.45
Material combination 3	226.44
Material combination 4	225.71

- Another important input for the SIMPACK model is the poisons ratio as described in the above table

CHAPTER 5: RESULT AND DISCUSSION

5.1 Wear analysis result, Wear number (Wear index)I_w

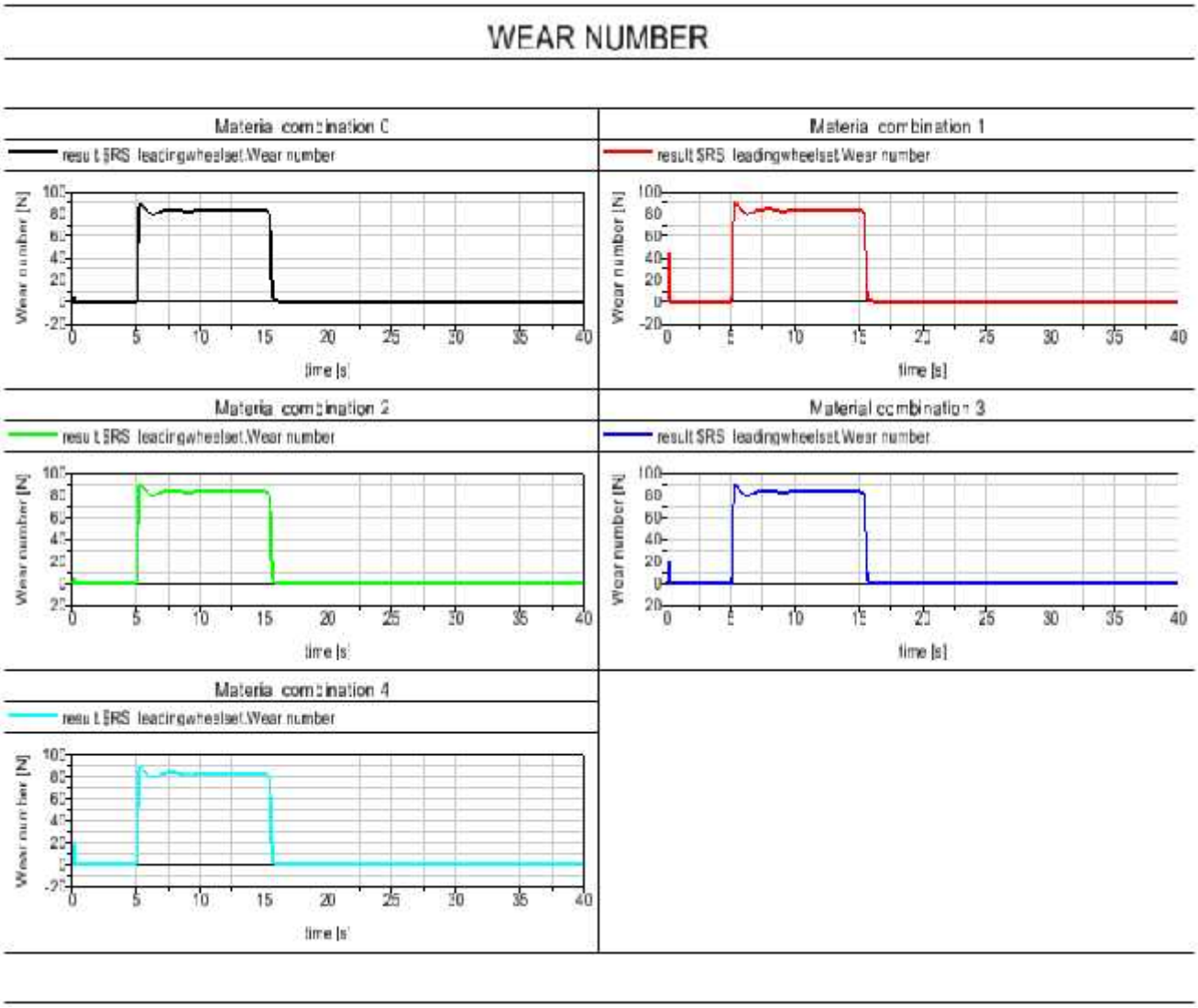

Figure 27: Wear results of the five material combinations using SIMPACK

5.1.1 Maximum wear number (wear index)

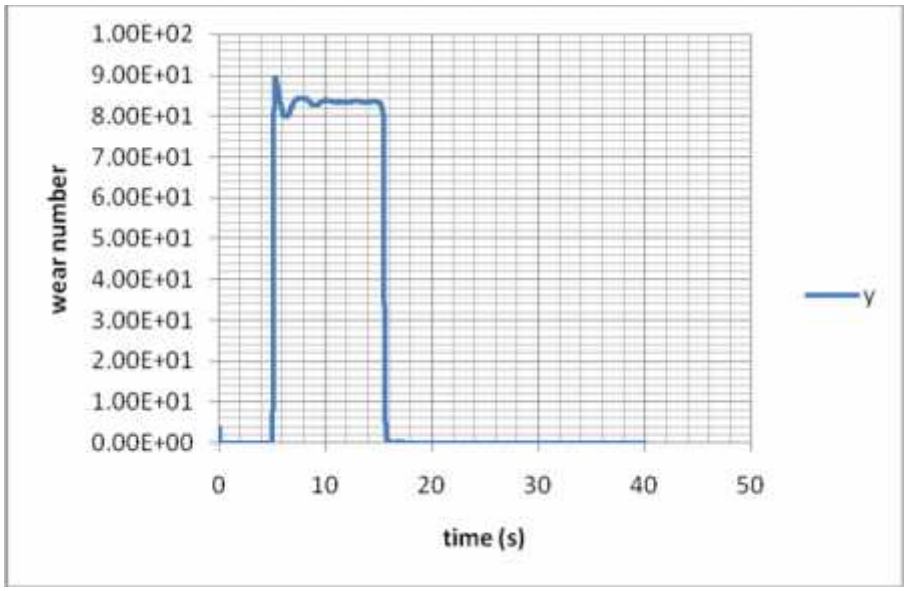

(a)

Number of values:	6001	
X Start:	0	Y Start:
X-End:	40	Y-End:
X-Min:	0	Y-Min:
X-Max:	40	Y-Max:	80.2608

	X	Y
1	0	
2	0.005	0
3	0.01	
4	0.015	0.0563859
5	0.02	0
6	0.025	0
7	0.03	0
8	0.035	0
9	0.04	0
10	0.045	0
11	0.05	0
12	0.055	0
13	0.06	0
14	0.065	0
15	0.07	0
16	0.075	0

(b)

Figure 28: Maximum wear number for material combination 0, (a) graphical representation and (b) SIMPACK output

Table 9: Maximum wear number of the five material combinations

Material combination	Wear index (Iw),max (N/mm^2)
Material combination 0	89.2698
Material combination 1	89.7228
Material combination 2	89.8164
Material combination 3	89.6633
Material combination 4	89.3419

5.1.2 Wear rate calculation

- **Wear rate K_w (I_w) from equation (16)**

$$K_W(I_W) = \begin{cases} 5.3 * I_W, & I_W < 10.4\ N/mm^2 \\ 55.0, & 10.4 \leq I_W \leq 77.2\ N/mm^2 \\ 61.9 * I_W - 4723, & I_W > 77.2\ N/mm^2 \end{cases}$$

Table 10: Wear rate of the five material combinations

Combination	Wear rate, K_w(µg/m mm^2)
Material combination 0	802.8
Material combination 1	830.8
Material combination 2	836.6
Material combination 3	827.1
Material combination 4	807.2

5.1.3 Specific volume of material removed

* From equation (17)

$$\delta_{p^j_{wL}(t)}(x,y) = K_w(I_w)/\rho$$

Where, ρ is density of wheel / rail material

$$\delta_{p^j_{rL}(t)}(x,y) = K_w(I_w)/\rho$$

Table 11: Specific volume of material removed

Combination	Specific volume of material removed ($mm^3/m\ mm^2$)	
	Wheel	Rail
Material combination 0	0.103	0.111
Material combination 1	0.107	0.106
Material combination 2	0.107	0.108
Material combination 3	0.105	0.106
Material combination 4	0.103	0.103

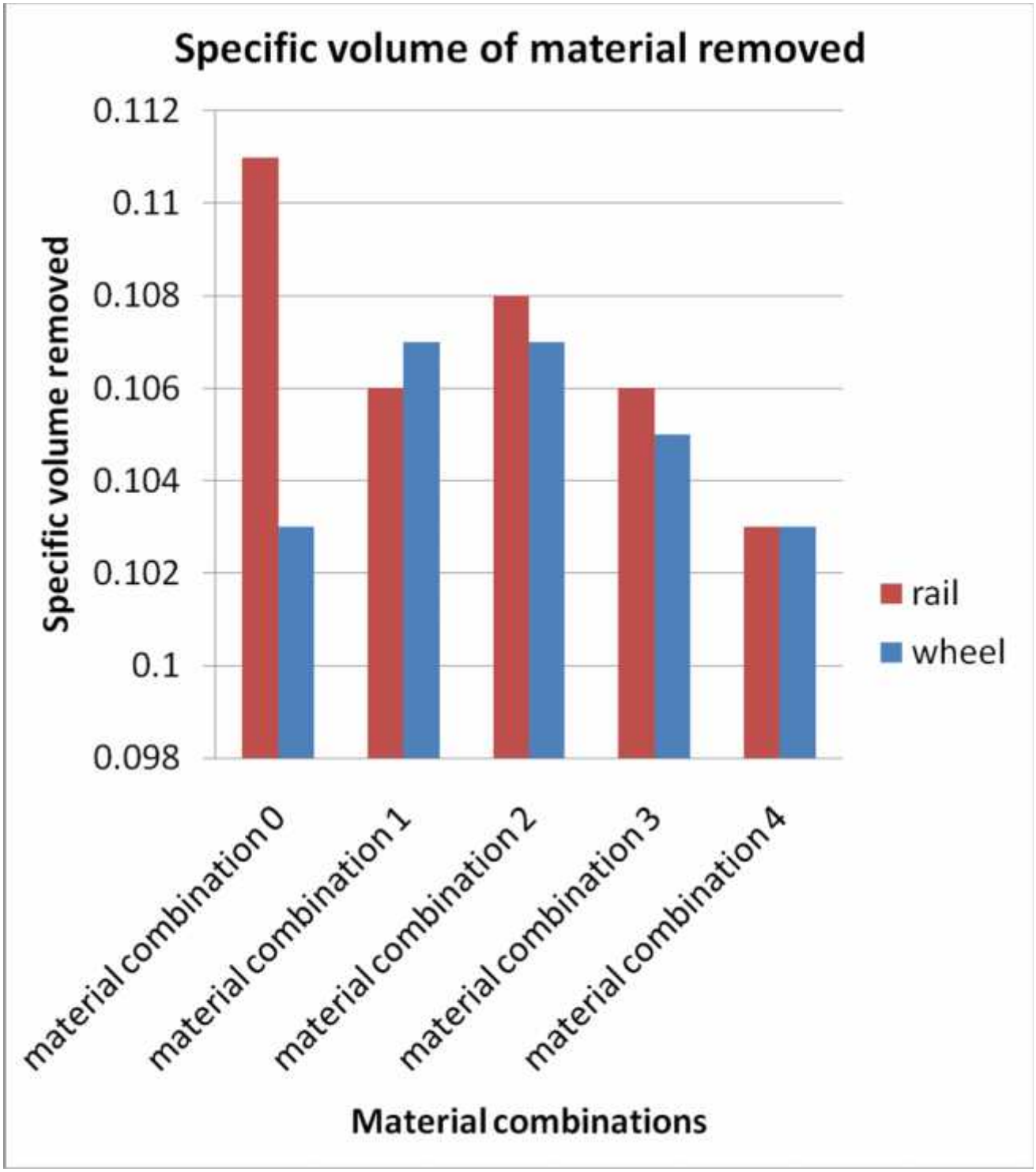

Figure 29: specific volume of material removed

5.2 Derailment coefficient

The derailment coefficient is an indicator of the risk of derailment of the vehicle. It indicates the safety level of the vehicle.

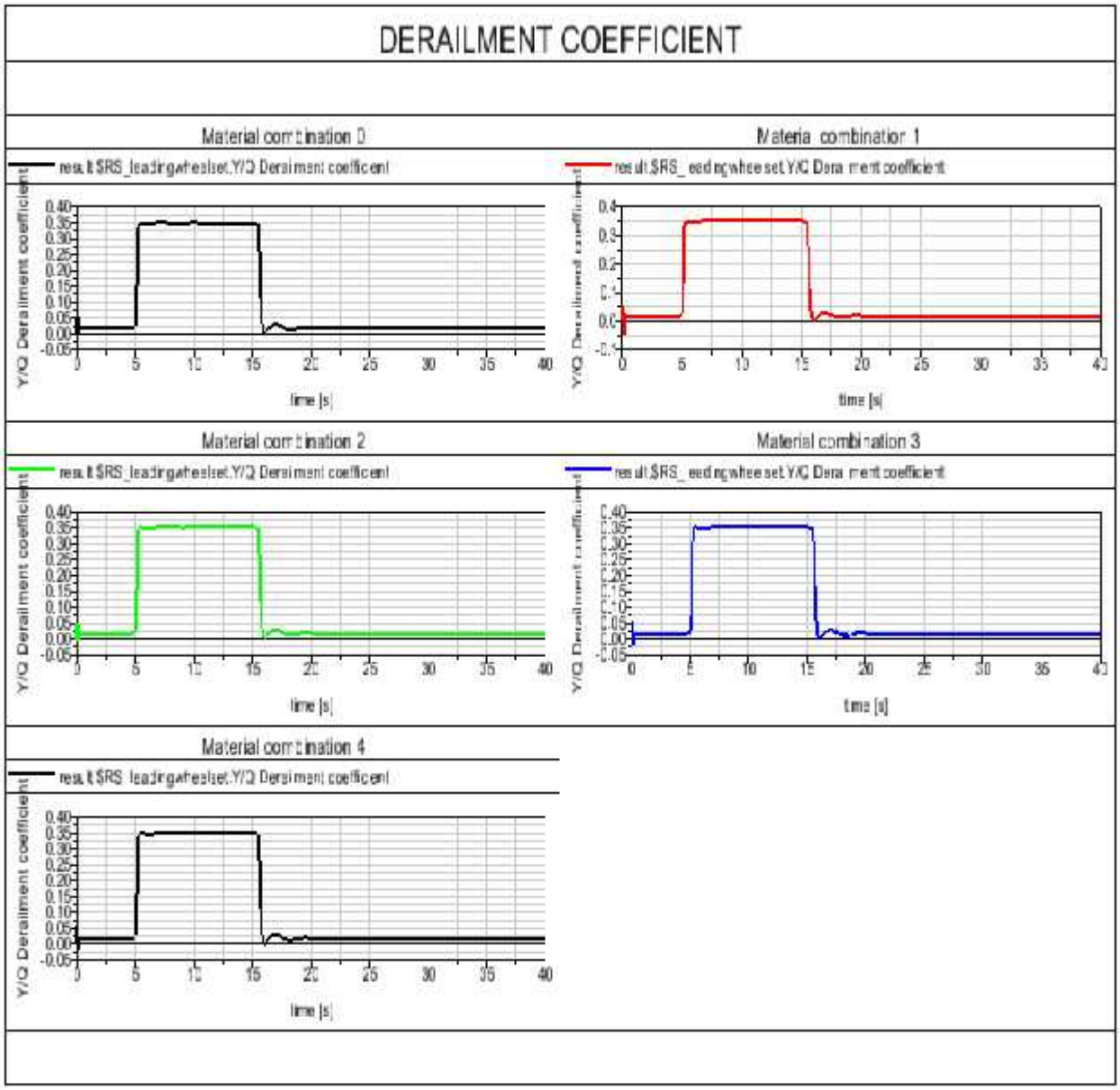

Figure 30: Derailment coefficient outputs

5.2.1 Maximum Derailment coefficient values

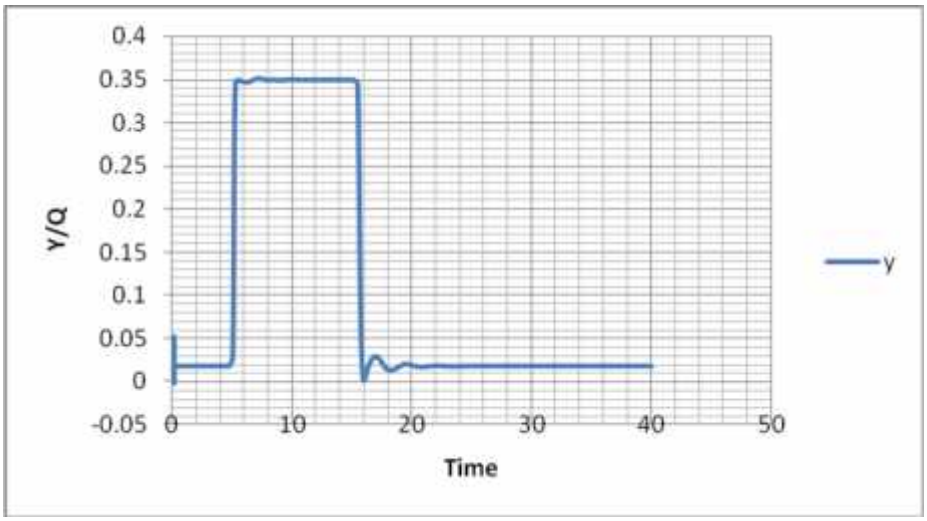

(a)

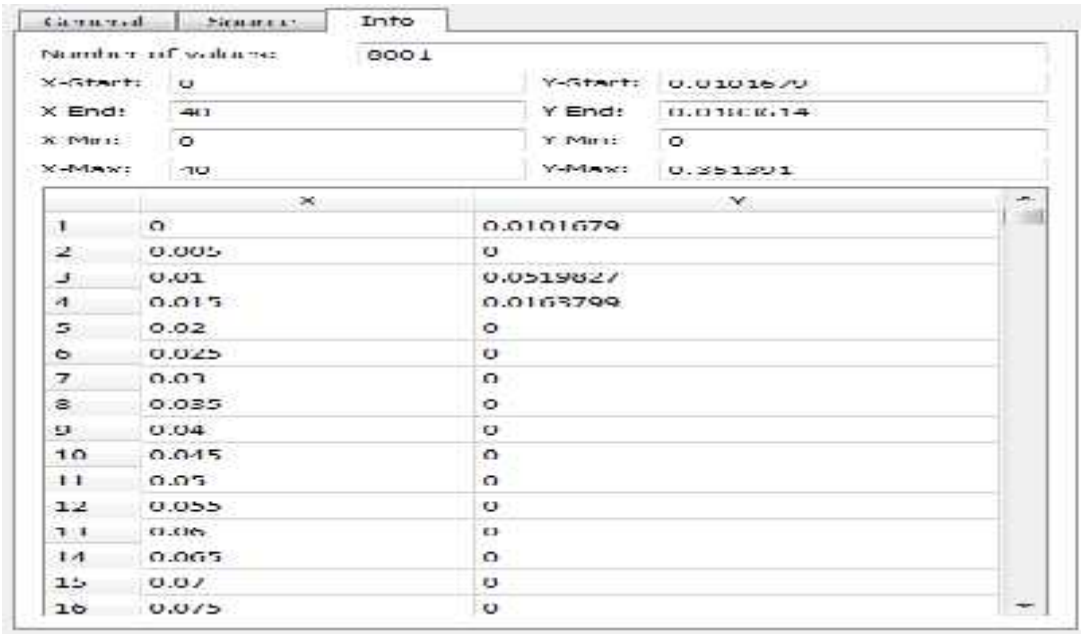

(b)

Figure 31: Maximum derailment coefficient of Material combination 0

Table 12: Maximum derailment coefficient values of the four material combinations

Combination	Derailment coefficient
Material combination 0	0.351391
Material combination 1	0.3530
Material combination 2	0.353967
Material combination 3	0.353946
Material combination 4	0.35176

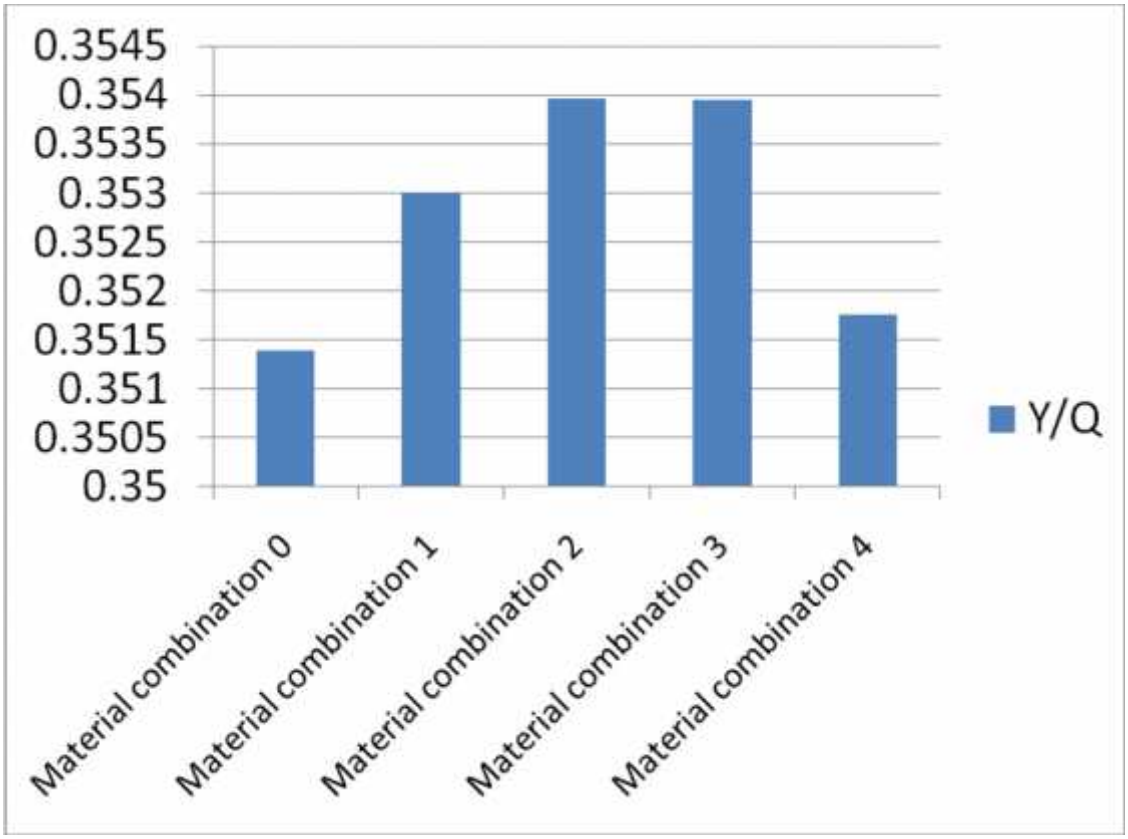

Figure 32: Maximum derailment coefficient of the five material combinations

5.2.3 Discussion on the derailment coefficient values

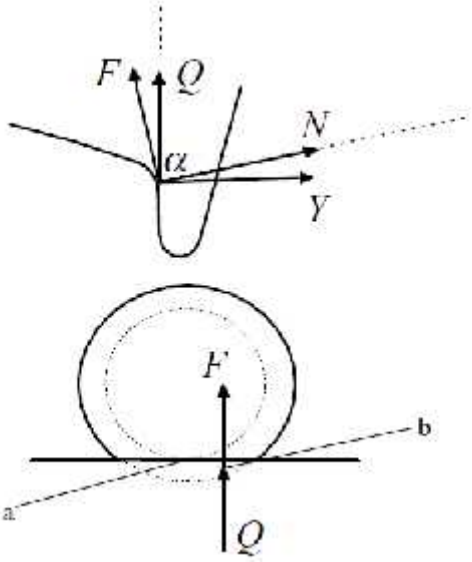

Q, vertical load
Y, lateral reaction
F, component of tangential force in the transverse vertical plane
N, normal reaction

Explanation

- Derailment occurs when the vertical load *Q* is carried entirely by the point of contact on the flange, and so the derailment limit is defined by the minimum value of the lateral reaction *Y*.

Figure 33: Forces at flange and tread contact [30]

$$\frac{Y}{Q} < \frac{N\tan\alpha - F}{N + F\tan\alpha}$$

- Y/Q is minimum when F is maximum
- F can't exceed μN

$$\frac{Y}{Q} = \frac{N\tan\alpha - F}{N + F\tan\alpha}$$

- We know that μ depends on the material in contact and it decreases as hardness increases. Which implies that the derailment coefficient is greatly affected by the hardness of the existiong material of the wheel and the rail as can be seen from the SIMPACK simulation and the mathematical equation.

CHAPTER 6: CONCLUSION, RECOMMENDATION AND FUTURE WORK

6.1 Conclusion

- Generally, as the hardness of the rail, increase there is a better wear performance but in the case of wheel rail contact a better result is obtained when a relatively softer wheel material rolls on a relatively harder material.
- Increasing hardness of both wheel and rail doesn't secure wear rate reduction
- Specific volume of material removed highly depends on the density of the material combination not only on hardness.
- Softer wheel material with rim heat treated perform better wear property when rolled on a harder rail.
- Grade of material also affects the coefficient of friction that is necessary to keep the vehicle on track.
- We can see that material combination 0 has the best wear performance for the wheel and material combination3 has the best wear performance for the rail. But the combined effect of the wheel from material combination0 and rail from material combination3 gives a better result. However, as the hardness increases the cost of material increases because of the processes needed to attain high hardness, which makes the initial investment, as well as replacement cost expensive.
- As a combination, among the simulated combinations material combination4 is the best in terms of wear performance and have a good stability in terms of derailment.

6.2 Recommendation

- From the results, we can see that material combination 4 has the best wear performance this material combination could be used for our countries railway transport.
- This research shows that material properties of the wheel and rail play a great role on the performance of the railway operation, and cost reduction. Due to this, heat treated materials like the rail material used in material combination 4 would bring a great benefit if used for our countries railway project.

6.3 Future work

- As a combination, material combination4 is better in terms of wear performance safety. But still the economical aspect in terms of initial investment cost, maintenance and replacement cost are not deeply studied. Due to this any interested researcher could perform further analysis in relation to cost and mechanical properties related to wheel rail contact and wear.
- As we can see from the paper there are lots of possible combination of wheel and rail materials throughout the world, it is only matching needed to get a new combination of wheel and rail materials . In this way, any interested researcher could do lots of tests using the test rig and software simulation in order to compare between these plenty of combinations and identify the best one suitable for the condition in need.
- The model of the rail vehicle developed in this paper could be used for future researches, being an easy ground especially if wheel/ rail contact related studies are made.
- We can't fully rely on software simulation results, due to this it is recommended to test all the five material combinations using the test rig equipment.

Reference

[1]. Roderick A Smith: "Railway and materials", vol 35, n^{o} 7, 2007, pp 505.

[2]. S. Marich: "Development of improved rail and wheel materials", pp 23-27.

[3]. MartinSchilke: "Degradation of Railway Rails from a Materials Point of View", 2013, pp3-9.

[4]. Cameron Lonsdale,Prof. Roman Bogacz,Mark Norton: Application of Pressure Poured Cast Wheel Technology for European Freight Service, world congress on railway research 2011.

[5]. Wolfgang Schoech, GregorGirsch, Rene Heyder:Advanced rail steel grades and their appropriate maintenance – the key to combat rcf, 2012.

[6]. "18thannual Association of American Railroad (AAR) research review", 2013.

[7]. www.amstedrail.com. | +1.312.922.4501 | 311 S.Wacker Drive, Suite 5300, Chicago, IL 60606. : The global leader in railway wheels, 2012.

[8]. Pombo, J., Ambrosio, J., Pereira, M., Lewis, R., Dwyer-Joyce, R., Ariaudo, C., Kuka, N. "A study on wear evaluation of railway wheels based on multibody dynamics and wear computation, Multibody System Dynamics", (2010) 24 (3), pp. 347-366

[9]. K. Mädler, A. Zoll, R. Heyder, M. Brehmer :"Rail Materials - Alternatives and Limits", Deutsche Bahn AG, DB Systemtechnik, Brandenburg-Kirchmöser, Germany

[10]. Venkatarami Reddy: Development of and Integrated method for assessment of operational risks in rail track.

[11]. 22nd International Symposium on Dynamics of Vehicles on Roads and Tracks (IAVSD2011), Manchester, UK, August 14-19, 2011

[12]. Benson, M. (1993) Effect of differential hardness on wheel/rail wear0 literature survey, BRR report LR MT 006, September 1993

[13]. Bolton, P. J. (1981) “Wear of six rail steels in rolling/sliding contact with Class D tyre steel. BRR report” TM MF 20, November 1981

[14]. McEwen, I. J. (1986) “A review of laboratory-based wheel on rail wear studies carried out by the vehicle track interaction unit. BRR report TR" VTI 003, March 1986

[15]. Singh, U. P., Singh, R. K. and Mangal, R. K. (1992) “Investigation of wheel and rail wear under conditions of sliding and rolling-sliding contact”. 10th International Wheelset Congress, Sydney, Australia, October 1992

[16]. Marich, S. and Curcio, P. (1978) “Development of high strength alloyed rail steels suitable for heavy duty applications. Rail steels developments, processing and use”, ASTM STP 644, 1978

[17]. The abrasive wear of wheel and rail steels and their inter dependence laboratory tests. British Steel Corporation Research Report SH/PROD/ENG/9422/-/81/B, April 1981.

[18]. Mädler, K., Zoll, A., Heyder, R. and Brehmer, M. (2001) “Rail materials alternatives and limits”. Proc. 8th World Congress on Railway Research (WCRR), Seoul, Korea, May 2008

[19]. Vasic, G. and Franklin, F. (2011) “Plastic deformation and crack initiation in hard pearlitic rail steels”. Proc. “21st Century Rail”, The Institute of Materials, Minerals and Mining, York, UK, November 2011

[21]. Katrin Mädler, Manfred Bannasch Deutsche Bahn AG, "Materials used for Wheels on Rolling Stock", Technical Centre, Brandenburg-Kirchmöser, GERMANY

[22] "Vehicle System Dynamics": International Journal of Vehicle Mechanics and Mobility Publication details, including instructions for authors and subscription information.13 Jun 2012.

[23]. J Santamaria, J. Herreros, E.G. Vadillo, N. Correa, "Design of an optimised wheel profile for rail vehicles operating on two track gauges" . Department of Mechanical Engineering. University of the Basque country UPV/EHU. Alameda Urquijo s.n., 48013 Bilbao, Spain.

[24]. Addis Ababa LRT Project North-South line project study report, China railway group limited, 2009.

[25]. David C. Grundy, B.S., *Fatigue and fracture of Railway wheel Steel,* University of Pittsburgh (1991).

[26]. "Design Technologies for Railway Wheels and Future Prospects", NIPPON Steel & Sumitomo metal technical report no. 105 December 2013.

[27]. "Modern Traibology Hand book". 2001,Chap. 34.

[28]. "Improved model for the influence of vehicle conditions (wheel flats, speed, axle load) on the loading and subsequent deterioration of rails", Newcast University,september 2006.

[29]. SIMPACK Documentation, Release 9.3, 2013.

[30]. A.H. Wickens, Fundamentals of Vehicle dynamics Guidance and Stability, University of UK, 2003

ADDIS ABABA UNIVERSITY

ADDIS ABABA INSTITUTE OF TECHNOLOGY

SCHOOL OF MECHANICAL AND INDUSTRIAL ENGINEERING

DECLARATION

I, the undersigned person, declare that this thesis is my original work and has not been presented for any degree in any university and all the sources of materials used for the thesis have been duly acknowledged.

Natnael Tesfamichael	_____	_____
Name	Signature	Date